

McGill University

Study of the Planetary Boundary Layer using GEM model simulations in
support of wind power projections for the Canadian Arctic

by

Caio Jorge Ruman

Department of Civil Engineering

McGill University, Montreal

March 2022

A thesis submitted to McGill University in partial fulfillment of the requirements of the degree of
Master of Engineering.

© Caio Jorge Ruman 2022

ABSTRACT

Temperature inversions are a common feature of the Arctic climate, affecting the surface energy budget and planetary boundary layer transports. The temperature inversion, in conjunction with the wind, is used to define the transition between two stable planetary boundary layer regimes, the weakly stable boundary layer, and the very stable boundary layer. This regime shift is sharply defined in terms of wind speed and temperature inversions, so accurate modeling of those two characteristics is crucial to a good representation of the Arctic climate.

This study investigates the evolution of large-scale temperature inversions in the context of a changing climate, in support of wind power projections for the Canadian Arctic. To this end, two five-member Regional Climate Model (RCM) ensembles, driven by the Canadian Earth System Model, spanning the 1950–2099 period, corresponding to two greenhouse gas emission scenarios (RCP 4.5 and 8.5), are considered. An ERA-Interim driven simulation for the 1979–2005 period is also considered to assess model performance.

A comparison of observed atmospheric soundings with the boundary layer variations in the reanalysis-driven simulation indicates that the model captures the temperature inversion characteristics reasonably well, with some positive biases in the temperature inversion strength and frequency. The transient regional climate change simulations suggest substantial decreases in both temperature inversion strength and frequency in winter in future climate for both emission scenarios. These changes are consistent with the reduced sea ice cover and the associated increase in cloud cover that reduce the surface radiative cooling necessary for the formation of strong temperature inversions. Some increases in the frequency and strength of temperature inversions are projected for summer over the Arctic Ocean, possibly linked with increased poleward moisture transport.

With the changes in the Arctic atmosphere seen in the future climate, the current predominant clear cold atmospheric state becomes less frequent. Cloudy and warm conditions that inhibit the formation of

temperature inversions become more common. This scenario will increase the frequency of the atmospheric regime where temperature inversions are weaker and the wind speed is higher, leading to increased wind power potential to the Arctic region and positive prospects to a transition to a clean energy regimen.

RESUME

Les inversions de température sont un phénomène usuel dans le climat Arctique qui affecte le bilan énergétique de la surface aussi bien que les transports de la couche limite planétaire. C'est l'inversion de température qui, combinée au vent, usuellement définit la transition entre deux régimes stables de couches limites planétaires, la couche faiblement stable et la couche très stable. Ce changement de régime est brusquement défini en termes de la vitesse du vent et d'inversion de température, donc la modélisation de ces deux caractéristiques est cruciale pour une bonne représentation du climat Arctique.

Cette étude se penche sur l'évolution en large escale des inversions de température dans le contexte des changements climatiques, afin de soutenir les projections d'énergie éolienne dans l'Arctique Canadien. Pour ce faire, sont considérés deux ensembles de cinq membres du Modèle Régional du Climat, piloté par le Système Terrestre Canadien, s'étendant entre 1950 et 2099, concernant deux scénarios d'émission de gaz à effet de serre (RPC 4.5 et 8.5). Une simulation pilotée par ERA-Interim pour la période 1979–2005 est aussi considérée pour évaluer la performance du modèle.

Une comparaison de sondages de l'atmosphère avec les variations de la couche limite dans les simulations pilotées de réanalyse ont indiqué que le modèle capture assez bien les caractéristiques de l'inversion de température, avec des quelques biais positifs dans l'intensité et la fréquence de l'inversion de température. Les simulations transitoires de changement climatique régional suggèrent des baisses significatives aussi bien dans l'intensité que dans la fréquence des inversions de température en hiver dans le climat futur dans les deux scénarios d'émission de gaz à effet de serre. Ces changements sont consistants avec la réduction de la couverture de glace des océans et l'augmentation associée de la couverture nuageuse qui réduit le refroidissement par radiation nécessaire à la formation des fortes inversions de température. Quelques augmentations dans la fréquence et intensité des inversions de températures sont projetées en été, probablement liées à l'augmentation du transport d'humidité vers les pôles.

Avec les changements dans l'atmosphère de l'Arctique prévus pour le climat future, l'état atmosphérique froid au ciel ouvert prédominant devient moins fréquent. Des conditions chaudes et nuageuses qui inhibent la formation des inversions de température deviennent plus communes. Tel scénario va augmenter la fréquence d'un régime atmosphérique où les inversions de température sont plus faibles et la vitesse du vent plus grande, menant à un potentiel éolien accru dans la région Arctique et des perspectives positives pour la transition vers un régime d'énergies propres.

ACKNOWLEDGMENTS

I would like to express my sincere gratitude and thanks to my supervisors, Prof. Adam Monahan and Prof. Laxmi Sushama for guiding me in this journey at McGill. They offered support when I needed it, encouragement, and patience to complete the work during COVID-19 times. I would also like to thank them for their financial support throughout this research.

I extend my gratitude to my lab colleagues, Bernardo Teufel, Vincent Poitras, Oleksandr Huziy, Gulilat Tefera Diro, François Roberge, Seok-Geun Oh, Tarek Dukhan, Katherine Zhao, Ju Liang, and Luis Duarte for the useful discussions we had, their assistance in preparing and extracting the data, and their valuable advice and insightful comments that made my work much easier.

Thanks to all the professors and staff members of the department of civil engineering and applied mechanics at McGill for their guidance. Finally, I would like to thank my family and my husband, Persio Witkowski Frangetto, for their support. This work would not have been possible without their unconditional support and continuous encouragement.

CONTRIBUTION OF AUTHORS

This thesis has been written following the requirements of Graduate and Postdoctoral Studies for a manuscript-based thesis. The main findings of the research undertaken by the author as part of his master's program are presented in a single manuscript. The author carried out the numerical analysis and wrote the manuscript under the supervision of Prof. Laxmi Sushama and Prof. Adam Monahan, his thesis supervisors. The publication detail is presented below:

- Ruman, C. J., Monahan, A. and Sushama, L. 2022. Climatology of Arctic temperature inversions in current and future climates (Submitted to the 'Theoretical and Applied Climatology' journal).

TABLE OF CONTENTS

ABSTRACT	2
RESUME	4
ACKNOWLEDGMENTS.....	6
CONTRIBUTION OF AUTHORS	7
LIST OF FIGURES	10
LIST OF TABLES	12
CHAPTER 1 INTRODUCTION.....	13
1.1. Background.....	13
1.2. Project Description.....	17
1.3. Objectives.....	17
1.4. Thesis outline	18
CHAPTER 2 LITERATURE REVIEW	19
2.1. Introduction.....	19
2.2. Planetary Boundary Layer and Temperature Inversions.....	19
2.3. Planetary Boundary Layer and Wind simulations	21
2.4. Climate Science and Artificial Intelligence	21
2.5. Environmental impacts of wind power generation in the Canadian Arctic	22
2.6. Knowledge Gaps and Conclusions	25
CHAPTER 3 CLIMATOLOGY OF ARCTIC TEMPERATURE INVERSIONS IN CURRENT AND FUTURE CLIMATES	26

3.1. Introduction.....	28
3.2. Model, Data, and Methods.....	30
3.2.1. Model.....	30
3.2.2. Observation Datasets and Reanalysis Products.....	32
3.2.3. Methods.....	32
3.3. Results.....	34
3.3.1. Climatology of the Temperature Inversions: Model and Observations	34
3.3.2. Climate Projections	39
3.4. Summary and Conclusions.....	45
CHAPTER 4 CONCLUSIONS AND RECOMMENDATIONS.....	48
4.1. Conclusions	48
4.2. Limitations and future research.....	49
REFERENCES	53

LIST OF FIGURES

Figure 1: Remote Community Migrogrids. Image from: (Knowles, 2016).....	13
Fig. 2 The Pan-Arctic experimental domain, with every fifth grid point shown. The inner bold line separates the blending and free zones.	31
Fig. 3 Spatial plots showing 2m temperatures for the 2003-2015 period for: GEM-ERA simulated climatological winter (a) and summer (b); CRU (land) and AIRS (ocean) winter (c) and summer (d); ERA-Interim winter (e) and summer (f). Differences between GEM-ERA and CRU/AIRS 2m temperatures for winter (g) and summer (h), and differences between GEM-ERA and ERA-Interim for winter (i) and summer (j).	36
Fig. 4 GEM-ERA simulated winter (a) and summer (b) temperature inversion strength. Winter (c) and summer (d) differences between GEM-ERA and ARIS (ocean) and atmospheric soundings (circles over land) for the temperature inversion strength. e)-(h): same as (a)-(d) for the temperature inversion frequency.....	37
Fig. 5 Difference between GEM-ERA and GEM-CAN simulations in DJF for temperature inversion strength (left column) and inversion frequency (right column for the 1980-2005 period.....	39
Fig. 6 GEM-CAN simulated temperature inversion strength for DJF (a) and RCP 4.5 projected changes to DJF temperature inversion strength for the 2040–2069 (b) and 2070–2099 (c) future periods with respect to the current 1976–2005 period. (d)-(e): same as (b) and (c) but for RCP 8.5. Hatched regions show where projected changes are statistically significant with the two-sample t-test at the 5% significance level.....	40
Fig. 7 GEM-CAN simulated temperature inversion frequency for DJF (a) and RCP 4.5 projected changes to DJF temperature inversion strength for the 2040–2069 (b) and 2070–2099 (c) future periods with respect to the current 1976–2005 period. (d)-(e): same as (b) and (c) but for RCP 8.5.	40

Fig. 8: GEM-CAN simulated total cloud cover for DJF (a) and RCP 4.5 projected changes to DJF total cloud for the 2040–2069 (b) and 2070–2099 (c) future periods with respect to the current 1976–2005 period. (d)-(e): same as (b) and (c) but for RCP 8.5. 41

Fig. 9 GEM-CAN simulated temperature inversion strength for JJA (a) and RCP 4.5 projected changes to JJA temperature inversion strength for the 2040–2069 (b) and 2070–2099 (c) future periods with respect to the current 1976–2005 period. (d)-(e): same as (b) and (c) but for RCP 8.5. Hatched regions show where projected changes are statistically significant with the two-sample t-test at the 5% significance level..... 43

Fig. 10 GEM-CAN simulated temperature inversion frequency for JJA (a) and RCP 4.5 projected changes to JJA temperature inversion frequency for the 2040–2069 (b) and 2070–2099 (c) future periods with respect to the current 1976–2005 period. (d)-(e): same as (b) and (c) but for RCP 8.5. 44

Figure 11: Vertical profiles of the mean wind speed (in m/s) for two locations in Arctic Canada: Inuvik and Kuujjuaq, for the DJF period of 1986-2015. Colors indicate the percentage of each wind speed, and each altitude sums up to 100%. The white line plot indicates the centroids of the k-mean clustering analysis..... 51

LIST OF TABLES

Table 1: Subset of radiosonde values plus standard deviation for the temperature inversion strength (ΔT) and the temperature inversion frequency (FREQ), with corresponding values from the GEM-ERA simulation for summer and winter.	38
--	----

CHAPTER 1 INTRODUCTION

1.1. Background

Climate change is one of the biggest threats we face today. According to the IPCC, the warming since the second half of the 20th century is unparalleled in thousands of years and there is a consensus that this will increase in future climate if actions are not taken. The consistent warming of the atmosphere and ocean is also reflected in the declining snow cover, sea ice, glaciers, and rising sea levels. This phenomenon is even more perceived in the Arctic region, as the increases in atmospheric greenhouse gas (GHG) concentrations lead to an alarming escalation of the temperatures in the Arctic (Overland et al., 2019). The observed and projected annual average warming in the Arctic is more than double the global mean, and they are even higher in the winter months (Overland et al., 2019). This positive anomalous temperature change, known as the Arctic Amplification, is important for the global climate system, including implications for lower latitudes (Cohen et al., 2014) and socio-economic and ecological consequences for all regions affected by it (Gillett et al., 2008). Thus, it seems imperative that actions be taken to reduce GHG emissions. The energy sector is particularly important in this context, as replacing fossil-based fuels with renewable energy can greatly reduce GHG emissions.

Many communities in Arctic Canada rely on diesel generators for electricity generation (Figure 1),

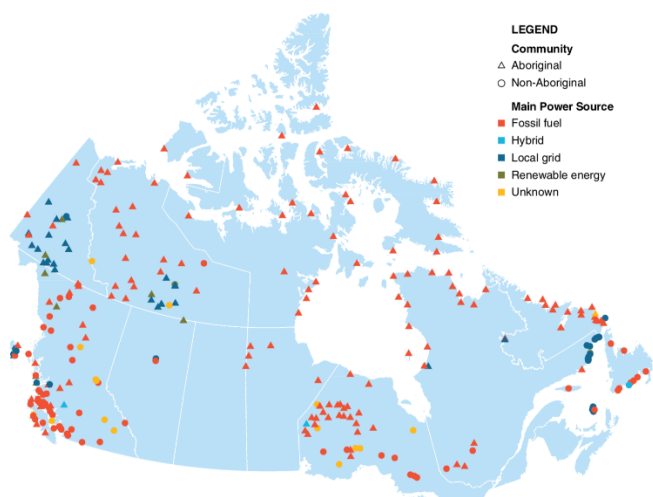


Figure 1: Remote Community Microgrids. Image from: (Knowles, 2016)

causing air pollution in an otherwise clean environment. Some communities are starting to think about how they can change the way they generate energy, going renewable, as shown in a series of strategic plans and energy assessments for the region (Generation Energy, 2018; Matangi, 2014; Pinard, 2016). Local renewable energy such as wind can substitute or reduce the

need for diesel generators in those communities. Inuvik recently got a plan approved to build the first wind energy farm in the Northwest Territories (NWT), which is expected to reduce GHG emissions by 30% (CBC News, 2018; Infrastructure Canada, 2019). Two companies that operate mines in Arctic Canada financed themselves wind power projects, with relative success. The first is the Diavik mine in NWT, built-in 2012, and the second is the Raglan mine in Northern Québec, built-in 2014 (Knowles, 2016). With this growing interest in wind energy, wind resource assessments for current and future climates are of utmost importance. Most wind-related studies have focused on southern regions of Canada (Daines et al., 2016; Richards et al., 2012; Werner, 2011), and more studies should be made to better understand wind characteristics for the Canadian Arctic.

Wind characteristics in the Arctic are different from lower latitudes as the Planetary Boundary Layer (PBL) in the region is predominantly stable, with characteristic wind profiles, having an impact on wind power generation due to lower-level jets and wind shear turbulence. Surface friction results in strong wind shears in the bottom several dozen of meters of the atmosphere; accordingly, the turbulence and wind power density also strongly vary with altitude (Dörenkämper et al., 2015; He et al., 2013; Mayfield et al., 2013). The character of this shear is determined by boundary-layer stability. Under conditions of unstable or weakly stable stratification, the shears are also relatively weak, and the turbulence is strong. In contrast, when the near-surface air is strongly stably stratified, shears are strong and turbulence is weak (Monahan et al., 2015). The character of stratification is determined by both large-scale and local processes and can change rapidly. Recent studies have emphasized the fact that the wind profile and stratification under stable stratification show two distinct states, or regimes, the weakly stable boundary layer (WSBL) and the very stable boundary layer (VSBL) (Monahan et al., 2015; Van de Wiel et al., 2017). The transition between those two regimes shows a distinct characteristic, where surface temperature inversions and wind speed play a crucial role. In the WSBL, the temperature inversion is weak and the wind speed strong, while in the VSBL the opposite occurs. Each stable PBL regime has its

own vertical wind profile, resulting in different values and optimum height for wind power generation. It is crucial to understand possible changes to the boundary layer characteristics in a changing climate, to better understand potential impacts on wind characteristics. This can be achieved by using global and regional climate models - more specifically the transient climate simulations developed using these models.

Global Climate Models (GCMs) coupling atmospheric, terrestrial, ocean and sea-ice components of the Earth System constitute the most comprehensive tools to make climate-change projections. GCMs have demonstrated considerable skills at reproducing the planetary and continental-scale features of the general circulation of the atmosphere and ocean. Operational GCMs use relatively coarser computational meshes compared to Numerical Weather Prediction (NWP) models, due to their high computational costs, resulting from the complexity of GCMs' components, the slow adjustment of the deep ocean, and the need for ensemble simulations for statistical significance. As a result, the resolution of common GCMs is not adequate for representing several key regional and local climate processes (Laprise, 2008; Rummukainen, 2010), or to satisfy the expectations of the climate impacts and community adaptation. Dynamical downscaling using nested limited-area models (LAM) known as Regional Climate Models (RCMs) allows the usage of meshes one order of magnitude finer over a region of interest, at an affordable computational cost. Hence, RCMs are used to 'add details' to GCM simulations (Feser et al., 2011) and to study climate and weather processes occurring at finer spatial scales. At higher resolution, geographical features become resolved as well as the effects they induce on local weather and climate.

For better comparisons between various studies as well as an easier communication of model results, it is preferable to use a common set of scenarios across the scientific community (van Vuuren et al., 2011). Representative Concentration Pathways (RCP) is the set of scenarios presently in use, and they describe different possible changes in GHG emissions and land use. Each RCP represents a larger set of scenarios, and they should be compatible with the full range of emissions scenarios available in the

current scientific literature, with and without climate policies. There are four RCP scenarios: one for heavy mitigation, leading to a very low forcing level (RCP2.6), two scenarios that stabilize the forcing at different points (RCP4.5/RCP6), and one very high baseline emission scenario (RCP8.5) without mitigation (van Vuuren et al., 2011). In this project, the RCP 4.5 and 8.5 scenarios are used. The RCP 4.5 has an aggressive but not improbable mitigation scenario (IPCC, 2013) in which at the end of the current century the global temperature rises slightly above the +2 °C global mitigation aim. The RCP 8.5 is a high-end scenario, where no mitigation is done due to the absence of policies on climate change, and GHG emissions continue to grow due to high energy demands (Riahi et al., 2011).

Projections of future climate are uncertain, firstly because they are dependent primarily on scenarios of future anthropogenic and natural forcings that are uncertain, secondly because of incomplete understanding and imprecise models of the climate system, and finally because of the existence of internal climate variability (IPCC, 2013). This uncertainty is exacerbated in the northern regions, due either to the lack of observations in those remote areas or by the different parameterizations used in those climate models.

The model used in this study, the Global Environmental Multiscale model (GEM) in limited area mode, has been used extensively for studying mechanisms and feedbacks in current and future climates (Diro & Sushama, 2017; Jeong & Sushama, 2018; Bernardo Teufel et al., 2019) and was validated for a series of climate variables (Teufel & Sushama, 2019), but the PBL was never fully studied. This work will investigate how the PBL is represented in GEM and how it can support wind power forecast and generation for the Canadian Arctic in current and future climates. To this end, temperature inversion characteristics in the GEM model are investigated first for the current climate, followed by an assessment of projected changes to these characteristics based on transient climate change simulations and a discussion of the implications of these changes to wind energy.

1.2. Project Description

This research is part of a MEOPAR Network (The Marine Environmental Observation, Prediction and Response Network) funded project on “Predicting the Future(s) of Renewable Energy in Canada’s Arctic”, aimed at producing and studying predictions of future wind and solar power resources in Northern Canada. The study is also part of the Year of Polar Prediction, an initiative of the World Meteorological Organization (WMO), that seeks to “enable a significant improvement in environmental prediction capabilities for the polar regions and beyond”.

This study will first assess the limitations of the GEM model, particularly in simulating the PBL and wind, using existing 50km horizontal resolution simulations for a Pan-Arctic domain. The simulations driven by re-analysis data (ERA-Interim) will be validated against observational datasets and reanalysis products, to understand biases. This will be followed by an assessment of projected changes, for RCPs 4.5 and 8.5, to the temperature inversion strength and frequency, with a focus on the Canadian Arctic.

The results of the research will provide a better understanding of the PBL characteristics and their projected changes, which are important for the development of wind power projects, to produce better weather forecasts, and to understand how the Arctic lower atmosphere behaves in a transient warming climate.

1.3. Objectives

The main research problem is to assess boundary layer-wind interactions in GEM for high-latitude applications, as relatively little work has been done so far in determining how well the model simulates the boundary layer in the Arctic environment.

The main objectives of this study therefore are:

- 1) Identification of model (GEM) deficiencies in simulating boundary layer characteristics for high latitude regions.

2) Development of projected changes to boundary layer characteristics, focusing on the temperature inversion strength and frequency, and how it can impact wind power generation in the Canadian Arctic.

1.4. Thesis outline

The thesis herein is divided into four chapters. A general overview discussing the background of the study area and objectives of this research is presented in the initial sections of Chapter 1. Chapter 2 reviews the existing literature surrounding temperature inversion characteristics, previous studies related to climate change in the Arctic, and environmental challenges for wind power projects in the Canadian Arctic. Chapter 3 is drawn from a journal paper, which analyzes the climatology of the Arctic temperature inversion characteristics in current and future warmer climates. Finally, Chapter 4 presents the summary of the findings and suggestions for future studies.

CHAPTER 2 LITERATURE REVIEW

2.1. Introduction

Climate modeling in the Arctic has been tackled through different angles in recent years, from uncertainty studies associated with the land surface model (Diro et al., 2014; Matthes et al., 2017), ocean heat transport (Mahlstein & Knutti, 2011), and precipitation (Rowell, 2012), to sensitivity studies of regional climate model simulations to different land surface process (Matthes et al., 2012; Bernardo Teufel et al., 2019) and resolution (Diro & Sushama, 2019; Leduc & Laprise, 2009; Roeckner et al., 2006).

Investigation of the Arctic climate using coupled general circulation models showed that uncertainties in modeling can arise from different emission scenarios, climate sensitivity, natural variability, climate feedbacks, and external forcings (Foley, 2010), and current climate models exhibit substantial uncertainties in the Arctic. This problem is especially challenging in the stably stratified boundary layer common in high latitudes, particularly in clear skies, wintertime, and low wind conditions at night (Holtslag et al., 2013) and its correct representation become harder due to the weak and intermittent behavior of turbulence (Mauritsen & Svensson, 2007).

2.2. Planetary Boundary Layer and Temperature Inversions

Recent stable planetary boundary layer studies focused on the transition of two stable PBL regimes, the weakly stable boundary layer and the very stable boundary layer (Monahan et al., 2015; Van de Wiel et al., 2017). This regime shift is sharply defined in terms of wind speed and temperature inversions, so accurate modeling of these two characteristics is crucial to a good representation of the Arctic climate. He et al. (2010) characterized the surface wind speed distribution and its dependency on land cover type, season, and time of the day based on observations, and used RCMs to determine how well the modeled surface wind speed distributions correspond to observations, and reported that the models failed to

reproduce the diurnal cycle of the wind distribution. Holtslag et al. (2013) reinforced the difficulty in representing the diurnal cycle, especially in the stable boundary layer, and noted that the coupling between the atmosphere and land surface is key to a good representation of the diurnal cycles. High-resolution simulations improve the coupling, as coarse resolution models fail to properly represent important coupled phenomena. The impact of the high-resolution simulations on the Arctic surface-based inversion will be studied for the first time in this thesis, as previous research on the subject used coarse resolution models (Medeiros et al., 2011; Wetzel & Brümmner, 2011; Y. Zhang et al., 2011) and they tend to overvalue the Arctic inversion strength (Boé et al., 2009; Medeiros et al., 2011)

The Arctic atmosphere is mostly stably stratified due to the polar night, where the radiative loss leads to frequent surface temperature inversions. Other forms of inversion formations in the Arctic include the advection of warm air masses, related to subsidence (Tjernström et al., 2019). When studying temperature inversions in the Arctic environment, some works (Wetzel & Brümmner, 2011; Y. Zhang & Seidel, 2011) follow the algorithm described by Kahl (1990), while others chose to compute the temperature difference between two levels (Bintanja et al., 2011; Medeiros et al., 2011). The surface temperature inversion has been suggested to cause negative feedback in the Arctic Amplification, enhancing the infrared radiative cooling (Boé et al., 2009), but new research shows that it acts as positive feedback, due to the ability of the Arctic wintertime clear-sky atmosphere to lose heat to space decreases with inversion strength (Bintanja et al., 2011).

Surface-based temperature inversions are an important aspect to better understand high-latitude climate change, as it is a constant feature of the Arctic Climate, mediating the surface energy balance and contributing to the Arctic Amplification as the GHG increases (Mark C. Serreze & Barry, 2006). The Arctic amplification was first predicted by climate models in 1980 (Manabe & Stouffer, 1980), and since that time this has been confirmed in other simulations (Bracegirdle & Stephenson, 2013; Holland & Bitz, 2003) as well as in reanalysis products (Cohen et al., 2014). Their causes include the albedo

feedback, sea-ice loss, horizontal heat-flux convergence, cloud cover, and water vapor and black carbon aerosols. One observed consequence of the Arctic amplification phenomena is the increase of the Arctic geopotential height due to the additional heat (Cohen et al., 2014). This increase in the geopotential height might reduce the poleward pressure gradient and lead to potential weaker storm tracks and westerly jets (Coumou et al., 2018).

2.3. Planetary Boundary Layer and Wind simulations

Studies about the projected changes in the wind speed using GCM show increased wind speed for central Arctic Canada, however not all the models used showed the same results (McInnes et al., 2011). Jeong & Sushama (2017) also found increased wind speed over Arctic Canada using an ensemble of RCM simulations but concluded that additional studies should be made using additional RCMs and driving GCMs to better quantify uncertainties. Furthermore, these studies were made with coarse resolution simulations, and the use of convection-permitting simulations (CPM) in the study of climate projections can facilitate the understanding of the climate system's behavior at scales most relevant to engineering applications and critical decision-making matters. Prein et al. (2015) indicate that CPM climate simulations are expected to better represent local features, as the improved representation of local topography and surface heterogeneities will have a significant impact on wind systems dominated by topography (Cholette et al., 2015) or feedback mechanisms like the soil moisture-precipitation feedback (Hohenegger et al., 2009).

2.4. Climate Science and Artificial Intelligence

A recent trend in the climate sciences is the use of artificial intelligence and machine learning to improve the prediction of events or to infer patterns in data, saving computational resources and producing better results. Machine learning techniques aim to complement and extend the use of

observations and climate models. It has been used to help predict extreme events, analyzing physical causes of extreme precipitation (Davenport & Diffenbaugh, 2021), and power outage events (Cerrai et al., 2020). Other uses include correcting the model error in data assimilation and forecast applications (Farchi et al., 2021), and parameterizing sub-grid processes in climate modeling (Yuval & O’Gorman, 2020). It is a promising area to explore in climate sciences. Sommerfeld et al. (2019) used a clustering analysis technique to differentiate the wind profiles based on the atmospheric stability, and this thesis discusses some preliminary ideas building on those principles, using machine learning techniques to automate the analysis of patterns in the wind profiles using the temperature inversions as the basis of differentiation of atmospheric stability.

2.5. Environmental impacts of wind power generation in the Canadian Arctic

With the current shift to the development of more renewable energy projects, it’s important to assess its environmental impacts, to make sure that they are indeed good to the environment and not just “to look green”. If the project is situated in the Arctic, it is paramount to proceed with care, as that region is rapidly changing due the climate change. Wind energy projects are big in scale, and the logistics for their implementation are not simple. The components for its construction are on a different scale, posing challenges for transportation to remote regions. This can impose new environmental challenges not considered when compared to similar projects in non-remote areas.

As wind energy generates minimal emissions during the operation phase, most of the environmental impacts are related to raw materials, manufacturing, and transportation (Alsaleh & Sattler, 2019). The main factories of wind turbine parts are in Europe, and the raw materials usually come from other parts of the world. To transport the turbines parts to the Canadian Arctic, the usual route is by ship, and after the parts arrive in the port, by ice road to the wind project locations. This makes the transportation of the components have a higher environmental impact when compared to other closer locations. Transportation to the Canadian Arctic is quite costly; Concrete, for example, is four times more expensive in the North,

at \$1,200/m³ versus \$300/m³ in the South (ecoENERGY Innovation Initiative, 2016). The company responsible for the Raglan mine wind project, Tugliq Energy Co., came up with an innovative solution, adapted to the Arctic conditions that reduce the costs and is environmentally friendly. Instead of a concrete foundation, they used a spider-like steel structure, that reduced the concrete used by 90%, making it impervious to the melting of the permafrost, and is more resistant, able to stand the Arctic blizzards (ecoENERGY Innovation Initiative, 2016). That approach to the materials flow of the project contributed to reducing the GHG emissions generated by transport and the use of concrete.

The recycling of wind turbines is an essential factor to reduce the environmental impact, as the materials used for manufacturing accounts for 75 to 85% of it (Alsaleh & Sattler, 2019; Kumar et al., 2016). Because of this, recycling is of economic and environmental importance, and in accordance with the principles of transitioning to a circular economy (Jensen, 2019). Closing the material loop has a positive impact on the use of natural resources, emissions, and energy use.

As the bulk of it comes from raw material acquisition and manufacturing, improving the flow of materials would certainly reduce the environmental impact. Moving the manufacturing to Canada or the US and using raw materials that do not require long-distance transportation are two proposed alternatives to reduce emissions. Reducing the emissions from installation and transportation can be hard, maybe impossible, due to the remote location of the Canadian Arctic, however different modes of transport can be used with the objective of reducing the environmental impact.

From a climate change perspective, there are a couple of issues that can arise in wind energy projects. The warming climate brings problems, like the melting of permafrost, erosion near the Arctic Ocean coast, and warmer winters. Ice roads are common in the region and are one of the only ways to transport heavy resources around. That is the case for the Diavik Mine, which makes the bulk of transportation during the short period when the ice roads are viable. With warmer winters, those ice roads aren't safe anymore, hindering transportation and increasing costs. The melting of permafrost is already bringing

issues to housing in Nunavut (Schreiber, 2018) and other Arctic communities (Natural Resources Canada, 2020), and it can make the installation of wind turbines even more costly, or unviable on certain Arctic terrains. However, one unexpected result of climate change might make wind projects more viable in the Arctic. Model projections of wind for the Canadian Arctic show that the wind speed is increasing in that region (Jeong & Sushama, 2017; Dukhan & Sushama, 2021), making wind power projects more desirable for the Canadian Arctic, especially for regions near the coast.

There are two successful wind projects in the Canadian Arctic, both showing that if the location has the wind resources to make it viable, wind power projects are a good solution to diminish the GHG emissions from the diesel generators used to provide electricity to the local communities. Both existing projects are able to reduce diesel consumption by 5-10%, and one of them, from the Raglan mine in Québec, is expanding (The Northern Miner, 2021). From the two local projects, the one of Raglan mine is the most promising to serve as an example to future projects in the Canadian Arctic. It has the lowest estimated environmental impact, proposing good solutions to reduce cost and non-recyclables raw resources. The current two projects in operation should be seen as examples to policymakers that they are viable in the Canadian Arctic. However, the recycling of their materials at the end of life is essential to truly negate their environmental impacts. Currently, there has been little policy action in Canada regarding the end-of-life of renewable technology materials flows or encouraging greater circularity of their materials (Cairns & Mccarney, 2021). There isn't much talk about it at the moment as most of the wind towers in Canada are still in operation, and it's estimated that they will start to be decommissioned only in 2030 (CanREA, 2021). Policies related to this must be created to prevent what happened around certain sites around the world, where the turbines were simply abandoned. The Canadian Arctic is a remote region, and it's costly to transport materials there and to bring them back. There is already a history of abandoned mines in Yukon and Northwest Territories (Crown-Indigenous Relations and

Northern Affairs Canada, 2020), and the two wind projects currently in the Arctic are on mines, turning on some red flags about the end-of-life aspects of those wind projects.

2.6. Knowledge Gaps

As presented in the sections above, climate models have difficulty in representing the Arctic planetary boundary layer, which has implications for wind resource assessments. Arctic temperature inversion strength and its frequency in particular and their wind linkages have not been adequately explored in the context of a changing climate using high-resolution regional climate simulations. This work addresses this knowledge gap through a detailed analysis of the Arctic temperature inversion strength and frequency using the limited version of the GEM model, which has been used extensively to study climate and climate change (Jeong & Sushama, 2019; Teufel et al., 2019; Oh & Sushama, 2020; Zhao & Sushama, 2020) for the region.

CHAPTER 3 CLIMATOLOGY OF ARCTIC TEMPERATURE INVERSIONS IN CURRENT AND FUTURE CLIMATES

C. J. Ruman¹, A. H. Monahan², L. Sushama¹

¹Department of Civil Engineering, McGill University

²School of Earth and Ocean Sciences, University of Victoria

Corresponding author:

Caio Jorge Ruman

Department of Civil Engineering

McGill University

817 Sherbrooke Street West, H3A 0C3

Montreal (Quebec) Canada

E-mail: caio.ruman@mail.mcgill.ca

ABSTRACT

Temperature inversions are a common feature of the Arctic climate, affecting the surface energy budget and planetary boundary layer transports. This study investigates the evolution of large-scale temperature inversions (between 925 hPa and 2m) in the context of a changing climate. To this end, two five-member Regional Climate Model (RCM) ensembles, driven by the Canadian Earth System Model, spanning the 1950–2099 period, corresponding to two greenhouse gas emission scenarios (RCP 4.5 and 8.5), are considered. An ERA-Interim driven simulation for the 1979–2005 period is also considered to assess model performance. A comparison of observed atmospheric soundings with the boundary layer variations in the reanalysis-driven simulation indicates that the model captures the temperature inversion characteristics reasonably well, with some positive biases in the temperature inversion strength and frequency. The transient regional climate change simulations suggest substantial decreases in both temperature inversion strength and frequency in winter in future climate for both emission scenarios. These changes are consistent with the reduced sea ice cover and the associated increase in cloud cover that reduce the surface radiative cooling necessary for the formation of strong temperature inversions. Some increases in the frequency and strength of temperature inversions are projected for summer over the Arctic Ocean, possibly linked with increased poleward moisture transport.

Keywords: temperature inversion, Arctic climate, climate change, regional climate modeling

3.1. Introduction

Temperature inversions, in which atmospheric temperature increases with height, are a frequent feature of the atmospheric boundary layer in the Arctic. The main temperature inversion formation mechanisms in the Arctic are surface radiative cooling (especially during the polar night), the advection of warm air masses over cooler surfaces, and large-scale subsidence warming in high-pressure situations. Consideration of temperature inversions is important to better understand high-latitude climate change, as they are a crucial feature of the Arctic climate, influencing the surface energy balance and contributing to Arctic amplification of anthropogenic climate change (Serreze and Barry, 2013). Each formation mechanism favors a different type of temperature inversion in the Arctic. Surface radiative cooling can lead to surface-based inversions and are more common in winter months, while large-scale subsidence and advection of warm air tend to form elevated inversions, commonly found in the summer. The temperature inversions can have varied types of structures, from simpler types to multiple inversions layers in the boundary layer, with a mix of surface-based and elevated inversions.

Arctic temperature inversions have been analyzed using data derived from satellites and radiosondes (Liu et al., 2006; Devasthale et al., 2010; Zhang et al., 2021), a combination of model simulations and radiosondes (Zhang et al. 2011), and climate models and reanalyses (Medeiros et al., 2011; Wetzel and Brümmer, 2011). Many studies have used the algorithm described by Kahl (1990) to compute the temperature inversion strength and height, and recently Fochesatto (2015) published a methodology for determining multilayered temperature inversions. Both methods require data from multiple layers in the lower levels of the atmosphere. In contrast, other studies have measured the temperature inversion by differencing temperatures between a selected pressure level above the planetary boundary layer (PBL) and either 1000 hPa or the surface temperature (e.g. Bintanja et al. (2011) and Medeiros et al. (2011)).

In the present study, we focus on the assessment of projected changes to large-scale Arctic temperature inversion characteristics, motivated by their important role in the Arctic climate. We use

regional climate model (RCM) simulations for two future emission scenarios and verify the model results using reanalysis, observations from radiosondes, and satellite data. As we are focusing on large-scale inversions in an RCM with a relatively coarse vertical resolution, multi-layer techniques such as those of Fochesatto (2015) cannot be used and the detailed structure of the temperature inversion structure is not resolved. As such, the present study defines the temperature inversion strength as the temperature difference between the 925 hPa pressure level and the 2m surface temperature. Estimating the temperature inversion strength by the temperature difference between two levels is a crude estimate of the temperature inversion strength, but reasonable when being used to analyze the large-scale structures and the stability of the lower troposphere in climate models which often have a coarse vertical resolution (Medeiros et al., 2011).

Most previous research has focused on winter temperature inversions, as they are more prevalent in that season due to the relatively strong radiative cooling. Summer temperature inversions' frequency and properties are much less dependent on surface net radiation and are largely regulated by the surface melt, poleward intrusion of warm air, and subsidence caused by the presence of polar high (Palo et al. 2017; Zhang et al. 2021). External forcings potentially have a stronger influence on the summer temperature inversion properties than local feedbacks. Most of the Arctic temperature inversion studies in the literature focus on present-day climatologies based on different models and reanalyses (e.g. Zhang & Seidel, 2011; Wang et al, 2020; Chang et al., 2021;). Few studies have investigated future changes in Arctic temperature inversions, with Zhang et al. (2021) focusing on the shallowing of temperature inversion depth and Koenigk et al. (2020) showing that the winter temperature inversion strength is greatly reduced in their work on the Arctic climate change in the 21st century. This study will be one of the first to investigate changes to temperature inversion strength and frequency in future climate projections for the Arctic.

The outline of this paper is as follows. The model, data, and methods used in this research are presented in section 2. Model assessment of temperature inversion characteristics and their projected changes are presented in Section 3. Conclusions are summarized in section 4.

3.2. Model, Data, and Methods

3.2.1. Model

The regional climate model used in this study is the Global Environment Multiscale (GEM) model (Côté et al., 1998) in a limited area mode (Teufel and Sushama, 2019). It has a non-hydrostatic dynamical core and uses the Arakawa C grid staggering in the horizontal and vertical coordinate based on hydrostatic pressure (Yeh et al., 2002). The numerical scheme is a two-time-level, semi-Lagrangian, implicit scheme. The GEM physics package includes: deep convection following Kain and Fritsch (1990), shallow convection based on a transient version of the Kuo (1965) scheme (Bélair et al., 2005), large-scale condensation (Sundqvist et al., 1989), correlated K solar and terrestrial radiation (Li and Barker, 2005), subgrid-scale orographic gravity wave drag (McFarlane, 1987), low-level orographic blocking (Zadra et al., 2003), and turbulent kinetic energy closure to estimate turbulent fluxes (Benoit et al., 1989; Delage, 1997; Delage and Girard, 1992). Lakes, both resolved and subgrid-scale, are represented by the Flake model (Mironov et al., 2010). The land surface scheme in GEM is the Canadian Land Surface Scheme (CLASS) (Verseghy, 2009), which allows a flexible soil layer configuration. CLASS includes prognostic equations for energy and water conservation for the soil layers and a thermally and hydrologically distinct snowpack where applicable.

This study uses two GEM ensembles of 5 members each, which are driven by five different members of a second-generation Canadian Earth System Model (CanESM2) initial condition ensemble, spanning the 1950–2099 period. The model experimental domain is displayed in Fig. 2. The two ensembles correspond to RCP 4.5 and 8.5 scenarios (van Vuuren et al., 2011). The RCP 4.5 has an aggressive but

not implausible mitigation scenario (IPCC, 2013) in which at the end of the current century the global temperature rises slightly above the +2 °C global mitigation aim. The RCP 8.5 is a high-end scenario, where no mitigation is done due to the absence of policies on climate change, and greenhouse gas emissions continue to grow due to high energy demands (Riahi et al., 2011). CanESM2 (Chylek et al., 2011) consists of the physical coupled atmosphere-ocean model, the Fourth Generation Coupled Global Climate Model (CanCM4), coupled to a terrestrial carbon model (CTEM) and an ocean carbon model (CMOC). The simulations driven by CanESM2 will be referred to as GEM-CAN hereafter. An additional ERA-Interim (Berrisford et al., 2009; Dee et al., 2011) driven simulation, named GEM-ERA, for the 1979–2015 period is used to assess the model's ability to simulate the temperature inversion characteristics based on available observations as discussed below. All model results presented below are ensemble means across the five ensemble members for each RCP.

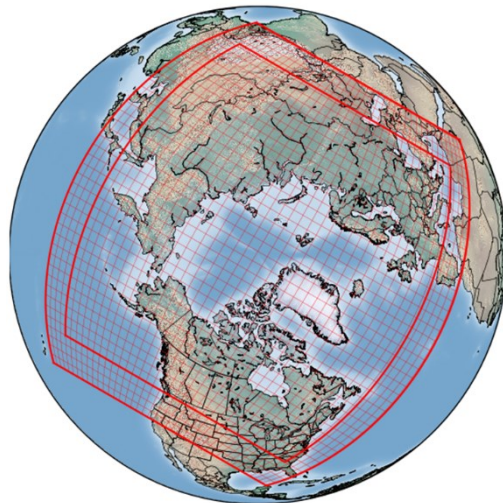


Fig. 2 The Pan-Arctic experimental domain, with every fifth grid point shown. The inner bold line separates the blending and free zones.

3.2.2. Observation Datasets and Reanalysis Products

The monthly averaged daily temperature dataset of the University of East Anglia Climate Research Unit (CRU, version TS 4.03; Harris et al., 2014) is used to assess model simulated temperatures over land. This dataset is available at 0.5° resolution and covers the global land surface. The Aqua/AIRS L3 Daily Standard Physical Retrieval V7 dataset - AIRX3STD (AIRS project, 2019), with 1° horizontal resolution is used to assess the simulated temperature and temperature inversion characteristics over the Arctic Ocean. The AIRS satellite has a sun-synchronous orbit, passing over the same location each day at 1h30 AM/PM local time (respectively the ascending and descending passes). Devasthale et al. (2010) showed that over the Arctic region, the difference in the temperature inversion strength is generally minimal between those two passes, so in this analysis, both passes were combined. The ERA-Interim reanalysis (Berrisford et al., 2009; Dee et al., 2011) is also used for the assessment of the 2m temperature. ERA-Interim is a global atmospheric reanalysis produced by the European Centre for Medium-Range Weather Forecasts (ECMWF) and covers the years from 1979 to the present time.

Observational radiosonde data from the Integrated Global Radiosonde Archive (IGRA) dataset (Durre et al., 2006) are used to assess model simulated temperature inversion strength and frequency. The radiosonde data are available twice daily (00UTC and 12 UTC) at more than 1500 locations around the globe, 153 of which are located inside the study domain. The IGRA data pass quality assurance algorithms, checking for format problems, climatological outliers, physically improbable values, and temporal and spatial discrepancies in temperature. Only stations with at least 80% of data during the 2003–2015 period are used for model assessment.

3.2.3. Methods

Before studying projected changes to temperature inversion strength and frequency, the ability of the model to simulate these are assessed by comparing GEM-ERA with available observations and reanalyses datasets. Reanalyses and satellite data provide a comprehensive set of data-informed climate

variables for such comparisons. Based on the study of three different reanalyses, Lindsay et al. (2014) identify ERA-Interim as the most consistent with independent measurements in the Arctic. ERA5 was not used in the GEM-ERA simulation as it was released after the model simulation was completed. The simulated 2m temperatures are assessed using CRU data, AIRS, and ERA-Interim reanalysis, while the temperature inversion strength and frequency are compared with atmospheric soundings available from the IGRA database and AIRS temperature profiles. The temperature inversion strength is estimated as the temperature difference between the 925 hPa level and the 2m temperature. Temperature inversion frequency is calculated as the ratio of the number of temperature inversion occurrences to the total length of the data record over the period of interest.

The AIRS satellite data is composed of satellite swaths, which have spatial and temporal sampling differences that can affect comparisons with climate models (Tian et al., 2013). To lessen this temporal and spatial bias, when assessing model data against the AIRS dataset, the model output was resampled hourly, and data were extracted from the model reproducing the satellite swaths on the model domain so that the spatial and temporal sampling of the model data is similar to that of the AIRS data.

Hearty et al. (2014) noted that the AIRS data sometimes report nonphysical temperatures near the surface over land, most notably near steep topography. For this reason, comparisons using the AIRS are only made over the oceans. Chang et al. (2018) found that the temperature inversion strength over the ocean is insensitive to cloud fraction variations, making it a good choice for model assessment. Over continental regions, the CRU dataset and the soundings were used instead. Plots using the AIRS data over the land can be found in the supplementary material (Figure S1).

Projected changes to the temperature inversion characteristics and 2m temperature for RCP4.5 and 8.5 scenarios are investigated by considering spatial distributions of 30-year averages of two future periods, mid-century (2040-2069) and late-century (2070-2099), and their differences with the current

period of GEM-CAN simulations. The statistical significance of the projections is assessed with the two-sample t-test at the 5% significance level.

3.3. Results

This section is divided into two parts: 1) model assessment and climatology of the temperature inversions from model and observations and 2) future projections of temperature inversion characteristics. All results from the GEM-CAN simulations presented in this section are based on averages across the five-member ensemble.

3.3.1. Climatology of the Temperature Inversions: Model and Observations

Comparisons of model-simulated 2m temperatures with CRU (land), AIRS (ocean), and ERA-Interim for winter (DJF) and summer (JJA) are shown in Fig. 3. Comparison with CRU data indicates cold biases between -1 and -6 °C over Europe and West Asia for DJF, while warm biases are noted over the northeastern parts of Eurasia. A cold bias is also present over Northeastern North America (NA) and a warm bias over the Western and Northwestern NA. The pattern and values of the bias over North America are similar to those found by Šeparović et al. (2013) when analyzing a GEM simulation over the NA domain. The strong positive bias relative to the CRU temperatures over Northeast Asia and the negative bias over Greenland should be interpreted with caution due to the sparse network of observations over the Arctic region; the bias is not as strong when comparing the model to the ERA-Interim reanalysis. Over the ocean, GEM-ERA has a similar spatial bias for both AIRS and ERA-Interim, with a negative bias over the central Arctic of -1 to -2 °C (ERA-Interim) and of -2 to -3 °C (AIRS) and positive bias of 1 to 3 °C over the coastal region of Siberia and Alaska. For the summer months, the model shows a persistent cold bias of -1 to -6 °C compared to both CRU and ERA-Interim. This cold bias is most prominent in East-Central Asia and the eastern Canadian Arctic. Over the Arctic Ocean, GEM-ERA shows a negative bias of -1 to -2 °C when compared with AIRS and ERA-Interim. These biases

notwithstanding, visual inspection demonstrates that the means from each dataset are reasonably similar, and the model shows good capacity in simulating the temperature patterns for each season, with spatial variability similar to the biases. As the temperature inversion is strongly coupled with trends in surface temperature (Zhang et al. 2011), knowing the surface temperature bias can lead to a better understanding of the model simulation of the temperature inversions.

The next step in the assessment compares the surface temperature inversion strength and frequency in GEM-ERA with those of the sounding data over land and with those of the AIRS dataset over the ocean, again for both winter and summer. The spatial plots in Fig. 4 show the simulated temperature inversion strength and its frequency and the difference between model values and soundings and AIRS for the Pan-Arctic domain for the 2003–2015 period, with the radiosonde data represented by the filled circles.

Radiative cooling of the surface is one of the key processes responsible for surface-based temperature inversion formation, and therefore higher-latitude locations, particularly in Greenland, Alaska, Canada, and Eastern Siberian Russia, experience more frequent and more intense temperature inversions than lower latitude stations in winter. Across the radiosonde data, the highest temperature inversion frequency occurs in the Arctic Canada region and Siberia, and the highest temperature inversion strength occurs in the interior of Alaska and Siberia. The temperature inversions are stronger and more frequent in winter due to the polar night and the weakening of air-surface thermal coupling by snow cover (e.g. Van de Wiel et al., 2017).

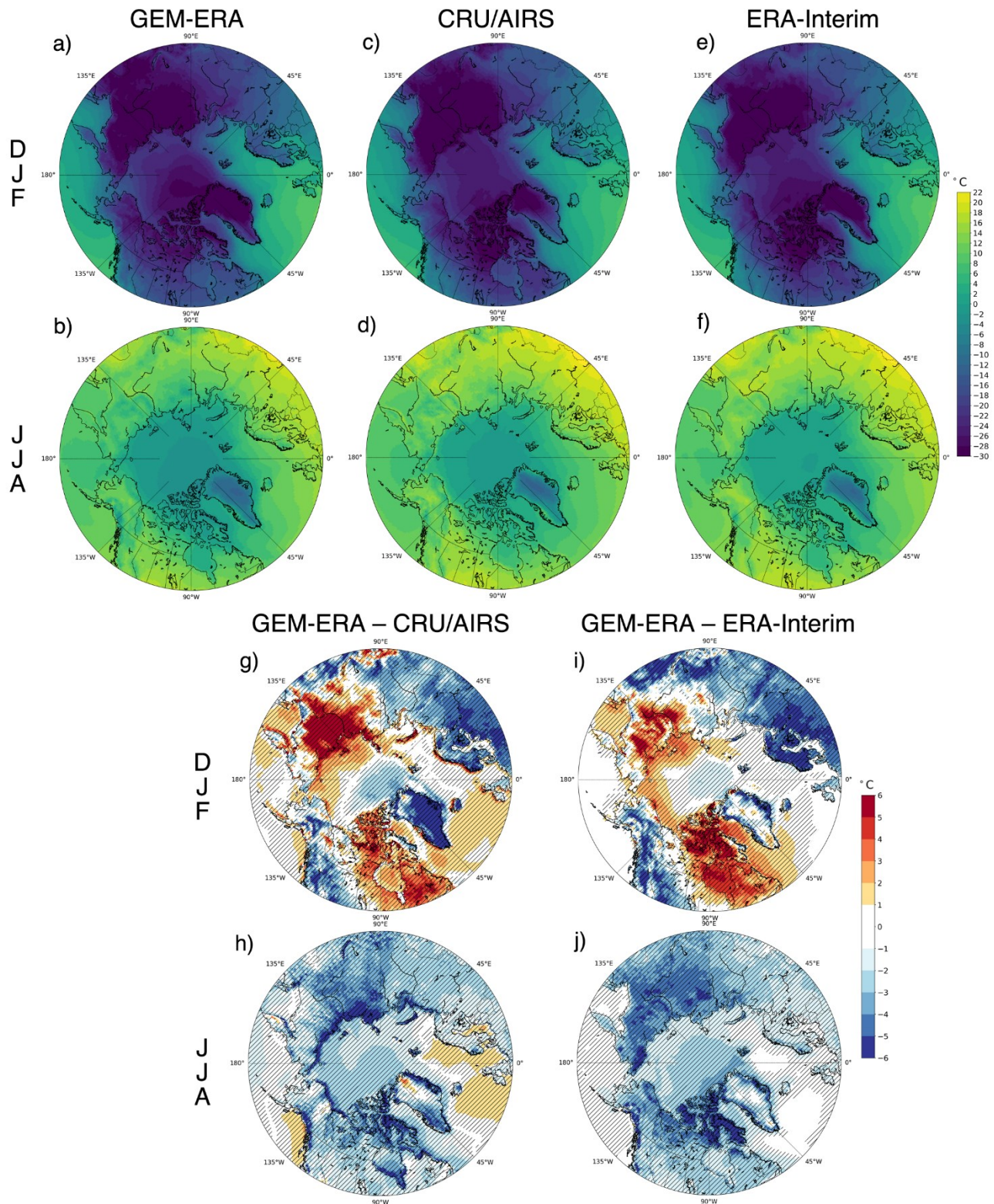


Fig. 3 Spatial plots showing 2m temperatures for the 2003-2015 period for: GEM-ERA simulated climatological winter (a) and summer (b); CRU (land) and AIRS (ocean) winter (c) and summer (d); ERA-Interim winter (e) and summer (f). Differences between GEM-ERA and CRU/AIRS 2m temperatures for winter (g) and summer (h), and differences between GEM-ERA and ERA-Interim for winter (i) and summer (j).

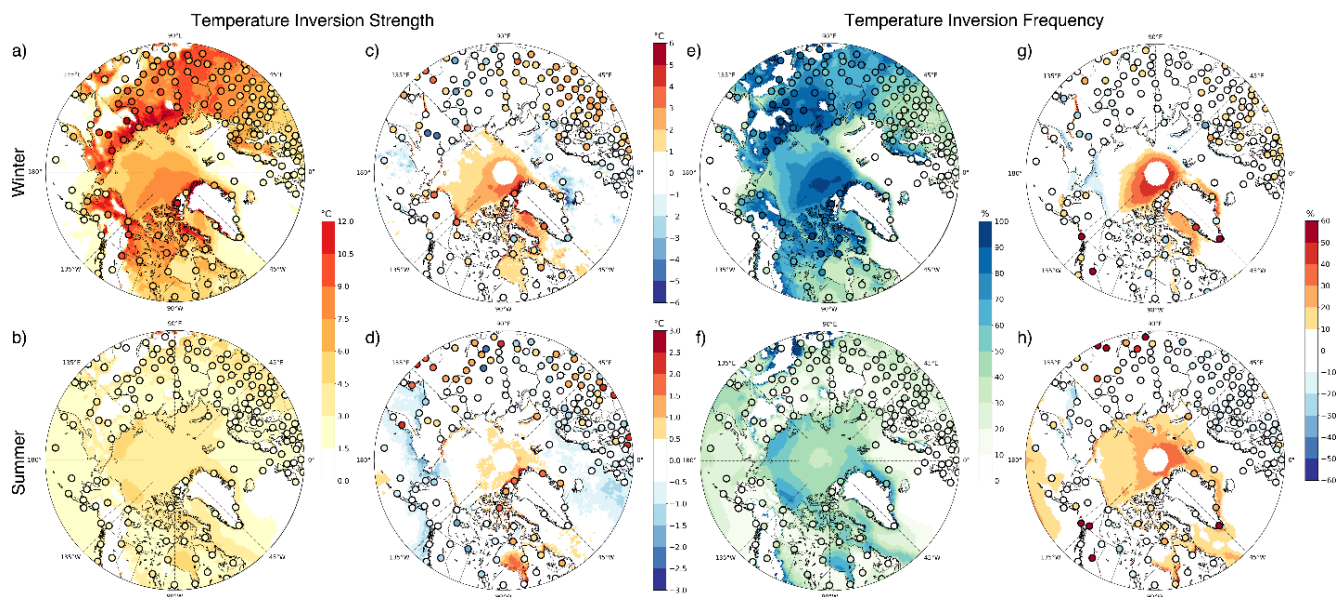


Fig. 4 GEM-ERA simulated winter (a) and summer (b) temperature inversion strength. Winter (c) and summer (d) differences between GEM-ERA and ARIS (ocean) and atmospheric soundings (circles over land) for the temperature inversion strength. e)-(h): same as (a)-(d) for the temperature inversion frequency. All plots are for the 2003–2015 period.

The patterns for the range of the temperature inversion strength and frequency values of North America (NA) are well represented in the simulation, with the largest winter inversion strength biases of 4°C occurring at a few coastal locations (three on the Arctic Ocean and one on west Greenland). Summer temperature inversion strength bias has a pattern of negative values ranging from -0.5 °C to -2 °C on the west NA and positive bias from 0.5°C to 2°C Nunavut, Quebec, and Greenland regions. Temperature inversion frequency has small differences, up to $\pm 20\%$ in both seasons, with a few outliers on coastal Greenland and the west NA Rockies region. The continental Eurasian patterns also show good agreement for both temperature inversion characteristics, with the winter temperature inversion strength showing positive biases of up to 3 °C in the European region and negative bias up to -4 °C in Siberia. Eurasian summer values do not show a defined pattern, with values ranging from -1.5 °C to 2 °C. Over the Arctic Ocean in winter, the GEM-ERA simulation has stronger and more frequent temperature inversions, limited to the region north of NA and the Baffin Bay. Summer produces a small positive bias of up to 1 °C for the temperature inversion strength and up to 20% for the temperature inversion frequency over

the Arctic Ocean. The model overrepresents the winter and summer frequency of the temperature inversion in the center of the Arctic Ocean, showing up to 50% more inversions in winter and 30% more inversions in the summer.

Table 1 shows the radiosonde values and standard deviation with corresponding values from the GEM-ERA simulation for summer and winter at eight locations above latitude 60° selected as the two best and worst results for each positive and negative winter bias of the temperature inversion strength. Results show good agreement between radiosondes and model values, as all model values are within the soundings' one standard deviation range. Overall, the spatial patterns of the temperature inversion strength and frequency from the GEM model are broadly in agreement with the results obtained from the radiosondes and AIRS for both seasons considered, with the largest differences occurring at a few stations in mountainous regions or the Greenland region. The results from the model display patterns and magnitudes that are broadly in accordance with the soundings for the Arctic region, for both seasons.

Table 1: Subset of radiosonde values plus standard deviation for the temperature inversion strength (ΔT) and the temperature inversion frequency (FREQ), with corresponding values from the GEM-ERA simulation for summer and winter.

Location (lat, lon)	DJF				JJA			
	Soundings		GEM-ERA		Soundings		GEM-ERA	
	ΔT (°C)	FREQ (%)						
ZYRYANKA (65.7, 150.9)	11.8±6.6	87	7.5±5.2	60	1.8±1.5	13	2.6±2.0	19
SEJMCHAN (62.9, 152.4)	9.4±5.1	79	5.2±4.3	51	3.2±2.2	25	3.8±3.1	29
SODANKYLA (67.4, 26.6)	7.9±6.1	53	7.5±5.2	66	2.7±1.9	21	1.8±1.5	8
OSTROV DIKSON (73.5, -80.4)	6.3±3.7	78	5.9±3.9	59	3.1±2.4	32	3.2±2.2	41
ARHANGEL'SK (64.6, 40.5)	5.1±3.8	44	5.2±3.8	42	2.6±1.8	23	1.4±1.2	8
BAKER LAKE (64.3, -96.1)	7.8±4.2	90	8.1±5.5	75	2.8±2.2	20	2.1±1.8	20
INUVIK (68.3, -133.5)	7.4±4.9	80	10.7±7.6	74	2.3±2	25	2.3±1.8	22
ALERT (82.5, -62.3)	5.8±4.0	82	9.5±5.9	84	3.0±2.1	43	4.5±3.1	52

When comparing the winter temperature inversion strength and frequency in GEM-ERA with those in GEM-CAN (Fig. 5), the main differences are over regions where the sea-ice concentration differs in the two simulations (not shown). This difference between the GEM-ERA and GEM-CAN simulations illustrates the strong relationship between sea ice and temperature inversion in higher latitudes. Pavelsky et al. (2011) showed that sea ice is the principal driver of spatial variability in inversion strength in the

Arctic Ocean. Besides the difference in regions where the sea-ice differs between simulations, the similarity of the two simulations demonstrates that driving by the GEM model does not increase the biases of simulated temperature inversions.

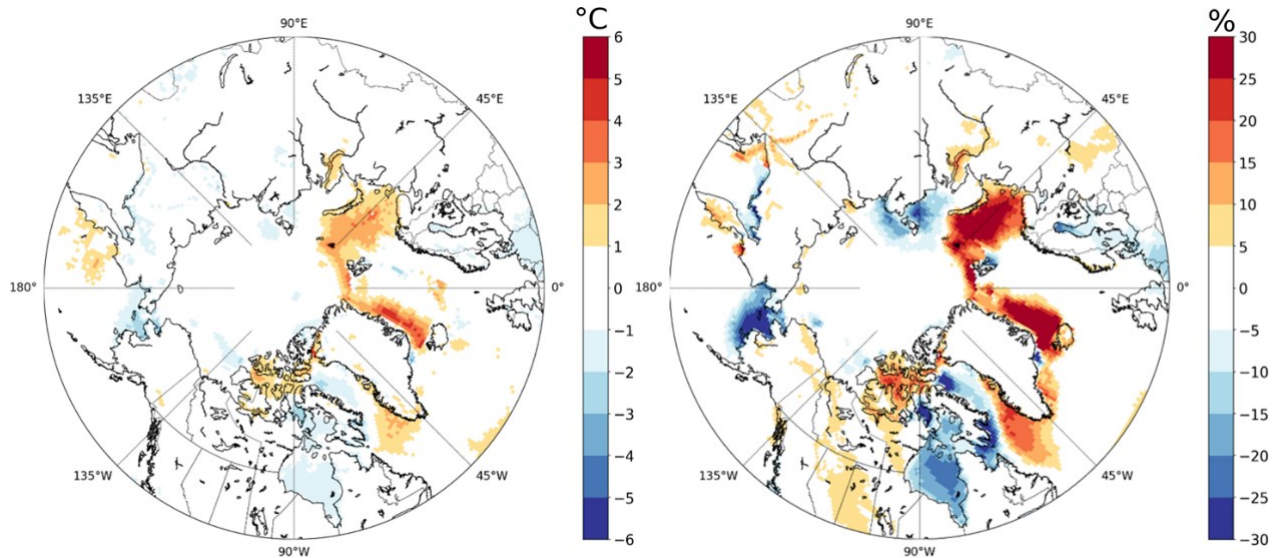


Fig. 5 Difference between GEM-ERA and GEM-CAN simulations in DJF for temperature inversion strength (left column) and inversion frequency (right column for the 1980-2005 period)

3.3.2. Climate Projections

Fig. 6 and 7 show the winter season's current climate (period 1976-2005) and projected changes of temperature inversion strength and frequency in the GEM-CAN simulation for the 2040–2069 and 2070–2099 future periods with respect to the 1976–2005 current reference period. Projections for RCP 8.5 indicate that winter season inversions will become weaker and less frequent, with the greatest change over the Arctic Ocean, where the temperature inversion strength is reduced by up to 5°C and 7 °C by the mid and late century, respectively. Over much of the Arctic Ocean, the temperature inversion frequency ranges from 60% to 100% lower for the 2070–2099 period than at present, with reductions of up to 100% in the ice-free regions, meaning that regions without sea ice lose the main contributor for temperature inversion formation in winter. Mid-century projected changes are milder, with most of the Arctic Ocean experiencing between 40 and 60% fewer temperature inversions, up to a 100% reduction in the Barents Sea.

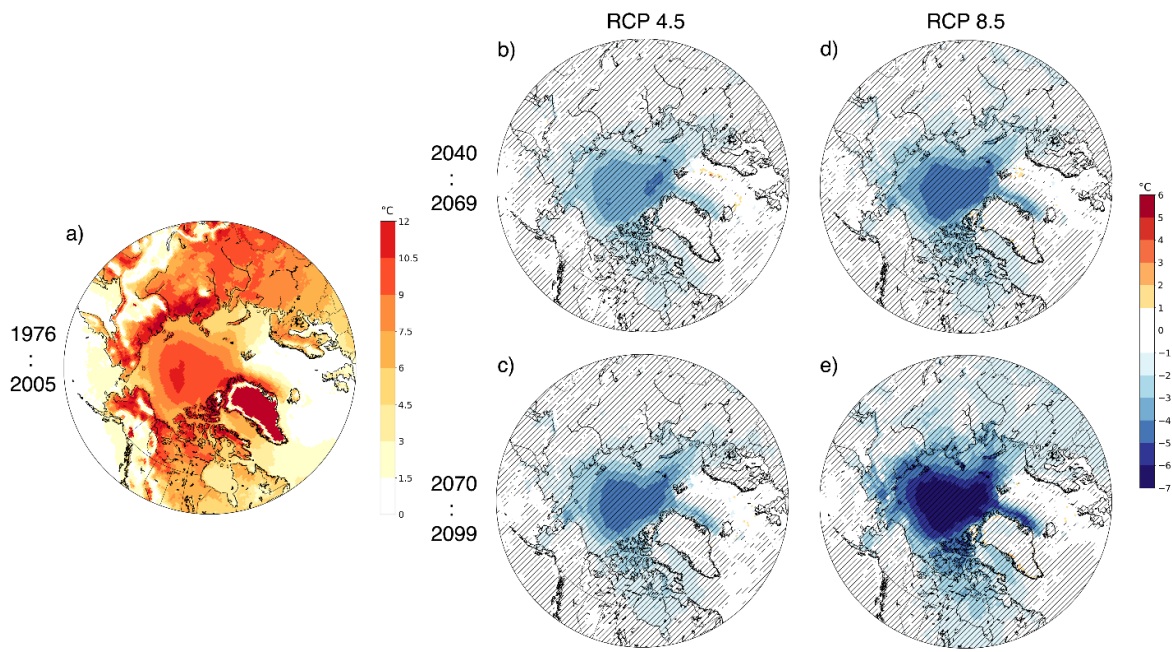


Fig. 6 GEM-CAN simulated temperature inversion strength for DJF (a) and RCP 4.5 projected changes to DJF temperature inversion strength for the 2040–2069 (b) and 2070–2099 (c) future periods with respect to the current 1976–2005 period. (d)–(e): same as (b) and (c) but for RCP 8.5. Hatched regions show where projected changes are statistically significant with the two-sample *t*-test at the 5% significance level.

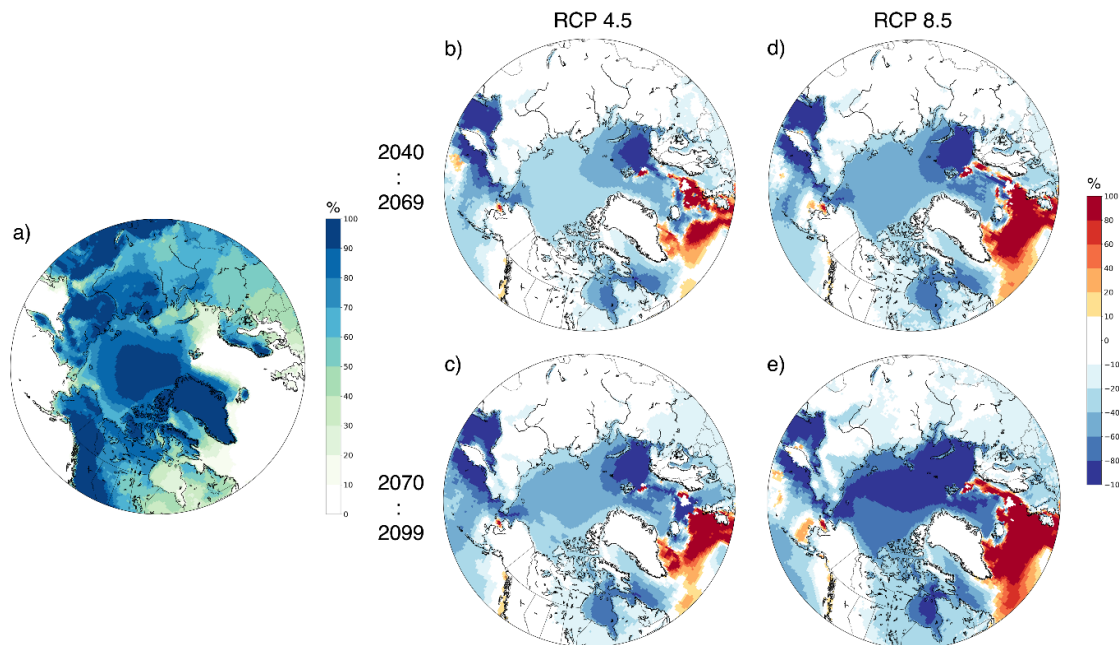


Fig. 7 GEM-CAN simulated temperature inversion frequency for DJF (a) and RCP 4.5 projected changes to DJF temperature inversion strength for the 2040–2069 (b) and 2070–2099 (c) future periods with respect to the current 1976–2005 period. (d)–(e): same as (b) and (c) but for RCP 8.5.

The changes in temperature inversion strength and frequency are consistent with the sea-ice loss and increased cloud cover in winter, with the Arctic Ocean becoming increasingly ice-free and cloudy as warming progresses. Wintertime overall cloud cover increases in all regions north of the 70° latitude, for both RCPs (Fig. 8). The increased cloud cover is consistent with the enhanced evaporation rates resulting from reduced sea ice cover (Boisvert and Stroeve, 2015). Increased ice-free areas in the summertime Arctic Ocean absorb more shortwave energy, resulting in increased latent heat flux later in the year (Morrison et al., 2019). As the main factor of strong surface-based temperature inversion formation over the Arctic is radiative cooling, the progressively ice-free ocean, the increase of cloud cover and surface temperature in winter favors a radiative-turbulent near-equilibrium state of the Arctic atmosphere characterized by a cloudy-sky state (e.g. Abraham and Monahan, 2019). The formation of temperature inversions is inhibited, and when temperature inversions occur, they are weaker.

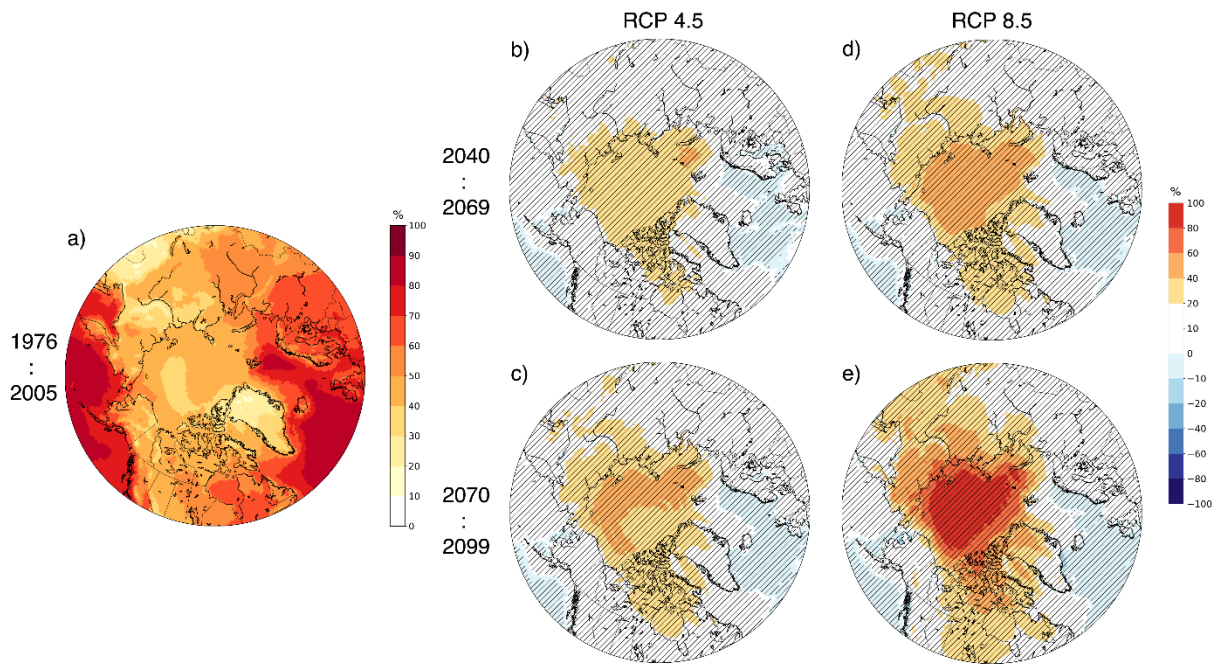


Fig. 8: GEM-CAN simulated total cloud cover for DJF (a) and RCP 4.5 projected changes to DJF total cloud for the 2040–2069 (b) and 2070–2099 (c) future periods with respect to the current 1976–2005 period. (d)-(e): same as (b) and (c) but for RCP 8.5.

The largest changes to temperature inversion properties are limited to the Arctic Ocean and adjacent water-covered regions. Only the simulations using RCP 8.5 show large spatial changes over continental areas, with less frequent and weaker inversions. The largest changes of temperature inversion strength over land are seen in the Canadian Arctic Archipelago and Northern Siberia for both future periods considered. The changes of temperature inversion frequency over the continents follow broadly the same pattern as that of temperature inversion strength, with changes in the inversion strength decreasing with increasing distance from the ocean. Lawrence et al. (2008) showed that the warming signal due to rapid sea-ice loss can penetrate inland, leading to terrestrial snow cover reduction changing the surface fluxes and planetary boundary layer characteristics (Alexander et al., 2010; Deser et al., 2010) that affect temperature inversion formation.

The RCP 4.5 simulations show similar patterns as RCP 8.5, but with less pronounced changes. For both the temperature inversion strength and frequency, the late 21st century for RCP 4.5 has similar spatial patterns and magnitudes of projected changes as the RCP 8.5 simulation in mid-century. The similarity is consistent with the corresponding RCPs warming signals due to increased CO₂ concentrations. For RCP 4.5, CO₂ stabilizes at ~500 ppm in the late 21st century. This value is reached by RCP 8.5 around mid-century. In the RCP 4.5 simulation, the late 21st century shows a 50% decrease of inversion frequency and inversions up to 5 °C weaker. Mid-century RCP 4.5 has temperature inversions up to 4°C weaker with a 30% reduction in temperature inversion frequency. The regions with complete loss of wintertime sea ice in the Arctic Ocean region show a 100% reduction of the inversion frequency in both periods.

Summer season values for the current climate and projected changes for the temperature inversion strength and frequency are shown in Fig. 9 and 10, respectively. For both RCPs, projected changes in the summer season show increased temperature inversion strength and frequency over the Arctic Ocean, except for the ocean regions of the Barents Sea and the Norwegian Sea. These regions show temperature

inversions up to 1.5 °C weaker, and up to 40% reduction in temperature inversion frequency, in both RCPs. The late 21st century in RCP 8.5 has up to 50% increased inversion frequency over the Arctic Ocean with inversion strength 1.5°C stronger. Except for the Ellesmere Island in the Canadian Arctic Archipelago, Arctic coastal regions show up to 40% fewer inversions, up to 2 °C weaker, with the southern region of the Canadian Arctic Archipelago having the most pronounced changes. The mid-21st century shows similar patterns as the late century, with weaker changes. These relatively large changes in temperature inversion frequency occur in regions in which summer temperature inversions are relatively common (> 40%) in the present climate.

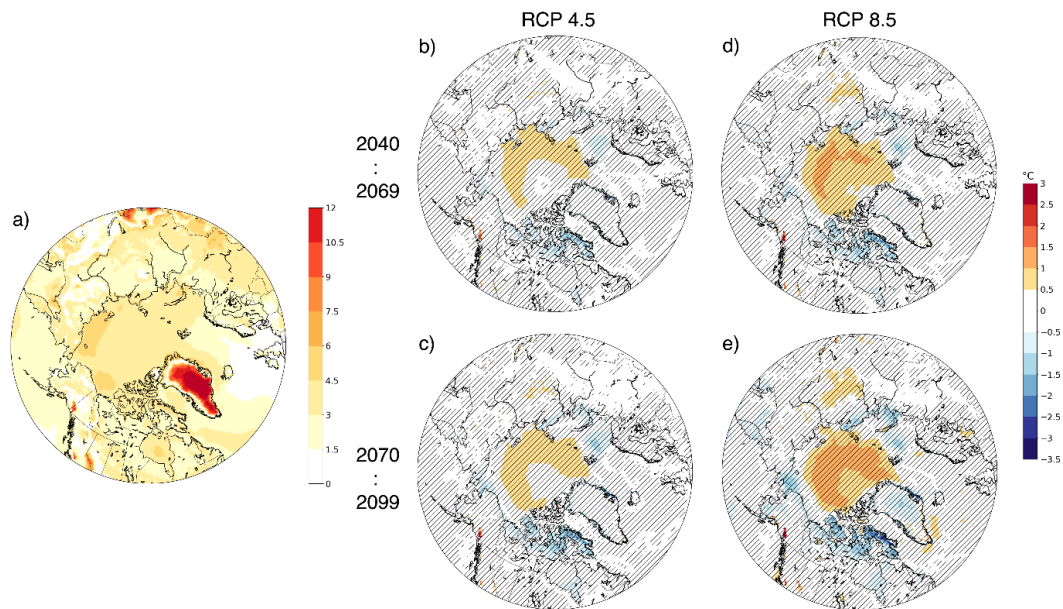


*Fig. 9 GEM-CAN simulated temperature inversion strength for JJA (a) and RCP 4.5 projected changes to JJA temperature inversion strength for the 2040–2069 (b) and 2070–2099 (c) future periods with respect to the current 1976–2005 period. (d)–(e): same as (b) and (c) but for RCP 8.5. Hatched regions show where projected changes are statistically significant with the two-sample *t*-test at the 5% significance level.*

Similar to the winter results, RCP 4.5 has the same pattern of changes as the RCP 8.5 for the inversion strength and frequency, but with smaller changes of both properties. The changes for the mid-century and late 21st century are similar, with the late century showing only slightly higher values. This can be explained by the stabilization of the climate in RCP 4.5 late 21st century.

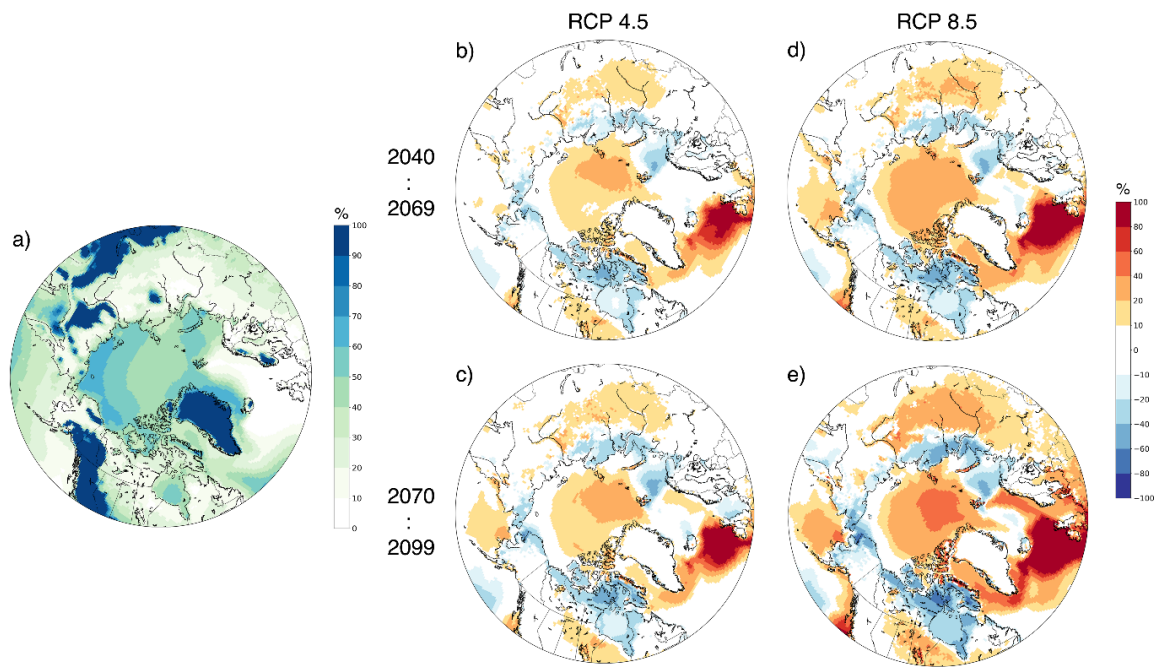


Fig. 10 GEM-CAN simulated temperature inversion frequency for JJA (a) and RCP 4.5 projected changes to JJA temperature inversion frequency for the 2040–2069 (b) and 2070–2099 (c) future periods with respect to the current 1976–2005 period. (d)-(e): same as (b) and (c) but for RCP 8.5.

The increase in strength and frequency of temperature inversions in summer is likely related to the increase in moist static energy transport in the Arctic, increasing the frequency of temperature inversion formation by advection of warm air masses over a cooler surface. Hwang et al. (2011) show an increase in poleward moisture transport in climate projections driven by the increased moisture as the climate warms. Tjernström et al. (2019) discuss the increased atmospheric water content in the Arctic due to the increased intrusion of warmer air masses, also causing strong surface temperature inversions due to subsidence in the summer months.

The results discussed above show the changes in temperature inversion characteristics for summer and winter. In winter, the main mechanism of formation is surface long-wave radiation cooling. Reduction in sea ice cover not only results in the loss of a cold surface but allows for increased moisture flux (Serreze et al., 2009; Screen and Simmonds, 2010a; Screen and Simmonds, 2010b;). The increased wintertime cloud cover reduces the surface longwave cooling rate, greatly diminishing the temperature

inversion formation by radiative cooling. For summer, subsidence and the transport of southern air masses likely drive the formation of temperature inversions.

3.4. Summary and Conclusions

In this study, climate projections of large-scale Arctic temperature inversion characteristics were investigated using an ensemble of the GEM climate model simulations for RCPs 4.5 and 8.5. This study includes the assessment of the model performance and characterization of the spatial distribution of the temperature inversion strength and frequency in summer and winter focusing on the large-scale structure of the temperature inversions, as the model cannot capture the fine-scale characteristics of the lower atmosphere.

The model slightly overestimates the temperature inversion strength and frequency in the current climate, consistent with the fact that numerical models have difficulty in representing the stable boundary layer, particularly in the Arctic (Fernando and Weil, 2010; Holtslag et al., 2013). For both summer and winter, the results from the model show patterns and magnitudes that are in overall accordance with soundings and the AIRS satellite data in the Arctic region. The spatial variability of the Arctic temperature inversions is strongly influenced by the surface type. In winter, ice-free zones in the North Atlantic have a low frequency of temperature inversions, in contrast with the sea ice-covered ocean and snow-covered regions where occurrence frequency exceeds 80%. Summer values of the temperature inversion frequency are higher for near-coastal regions (up to 70% frequency), in contrast to the central Arctic (40% frequency). Analyses of the transient climate change simulations indicate that the loss of sea ice and related increase in cloud cover in winter leads to weaker and less frequent temperature inversions. This reduction in the occurrence of very strongly stratified conditions is consistent with the reduction in surface radiative cooling resulting from increased cloudiness. The increase of cloud cover is associated with an increased surface moisture flux during the winter seasons after the mostly ice-free sea absorbed energy in the summer. For ocean regions in the summer, there is an increase in temperature

inversion frequency and strength at the end of the 21st century, consistent with an increase in poleward moist energy transport.

With the changes in the Arctic atmosphere seen in the future climate, the current predominant clear cold atmospheric state becomes less frequent. Cloudy and warm conditions that inhibit the formation of temperature inversions become more common. For the winter season, the reduction of sea ice and the increased cloud cover prevents the radiative cooling necessary to the formation of strong temperature inversions, and for the summer, the increased poleward moisture transport is likely due to increased synoptic-scale warm air advection over the cooler ice-free ocean causes a higher incidence of temperature inversions.

These results provide information about how large-scale temperature inversions are represented in climate models and about the effects of a warming climate in the Arctic planetary boundary layer, as changes in temperature inversion characteristics have important implications for the Arctic climate system. For example, temperature inversions mediate the surface energy balance (Bradley et al., 1992; Medeiros et al., 2011), restrict the vertical exchange of momentum, heat, moisture, and pollutants between PBL and the free atmosphere (Wetzel and Brümmer, 2011) and are an important contributor to Arctic Amplification (Bintanja et al., 2011). In this study, we analyzed Arctic temperature inversions looking at relatively coarse structures of the planetary boundary layer. Future work benefiting higher vertical resolution and better representation of near-surface processes could focus on simulating the changes of the more detailed vertical structure of the atmosphere.

Acknowledgments

This work was supported by funding from the Marine Environmental Observation, Prediction, and Response (MEOPAR) and Polar Knowledge Canada (POLAR). CJR acknowledges the support of the McGill Engineering Doctoral Awards (MEDA) program. AHM acknowledges the support of the Natural Sciences and Engineering Research Council of Canada (NSERC), [funding reference number RGPIN-

2019-04986]. The GEM simulations in this study were performed on supercomputers managed by Calcul Québec and Compute Canada.

CHAPTER 4 CONCLUSIONS AND RECOMMENDATIONS

4.1. Conclusions

In this work, the Arctic temperature inversion characteristics were studied using observational soundings data for the current climate, and an ensemble of GEM climate model simulations for current and future climates, with the latter corresponding to RCP 4.5 and 8.5 scenarios. It included the assessment of the model performance and characterization of the spatial distribution of the temperature inversion strength and frequency in summer and winter focusing on the large-scale structure of the temperature inversions.

The main findings related to model performance shows that it slightly overestimates the temperature inversion strength and frequency in the current climate. Those results are consistent with the problem that models have in representing the complexities of the stable boundary layer. When comparing the results from the model against observations from atmospheric soundings and the AIRS satellite data, summer and winter results shows good accordance with the patterns and magnitudes in the Arctic Region. The surface type has a strong influence in the spatial variability of the temperature inversions in the Arctic, as seen in winter in the low frequency of temperature inversions in the ice-free zones in the North Atlantic and high frequency in the sea ice-covered ocean and snow-covered regions. For summer, the temperature inversion frequency is higher near coastal regions, up to 70%, contrasting to the central Arctic, with only 40% frequency. This is due the transport of warm air masses over the colder Arctic Ocean, which causes the formation of temperature inversions near the coast. As the air mass moves further from the coast, it becomes well mixed, and the temperature inversion disappears.

The findings of this study on the transient climate change simulations indicate that the loss of sea ice and related increase in cloud cover in winter leads to weaker and less frequent temperature inversions in future climate. This reduction in the occurrence of very strongly stratified conditions is consistent with the reduction in surface radiative cooling resulting from increased cloudiness. For summer, the increased

poleward moisture transport, likely due to increased synoptic-scale warm air advection over the cooler ice-free ocean, causes a higher incidence of temperature inversions.

These results provide information about how large-scale temperature inversions are represented in climate models and about the effects of a warming climate in the Arctic planetary boundary layer, as changes in temperature inversion characteristics have important implications for the Arctic climate system. With the changes in the Arctic atmosphere seen in the transient climate change simulations, the current predominant clear cold atmospheric state becomes less frequent. Cloudy and warm conditions that inhibit the formation of temperature inversions become more common. This scenario will increase the frequency of the atmospheric regime where temperature inversions are weaker and the wind speed is higher, leading to increased wind power potential to the Arctic region and positive prospects to a transition to a clean energy regimen.

4.2. Limitations and future research

One limitation of this research is the coarse resolution of the GEM simulations. As the model has a 0.5° horizontal resolution (~ 50 km), it can have an inadequate representation and parameterization of sub-grid scale features, which are one of the main sources for uncertainties in regional climate change projections. Increasing model resolution to a couple of kilometers will be helpful in resolving some of these challenges, for example, to better simulate convection and refined land heterogeneity and thus land-atmosphere interactions. The second limitation is due the lack of observations in the northern regions, making it difficult to assess how good are the model simulations of those areas, increasing the uncertainty regarding the study in remote regions.

The results of high-resolution simulations are expected to produce significant improvements in the PBL and wind representation for Arctic Canada. Results from Diro & Sushama (2019) showed significant improvements in a high-resolution simulation over an Arctic domain covering Nunavut. The study focused on temperature and precipitation characteristics, and wind and PBL parameters were not

considered. This study indicates that some aspects of the seasonal mean values are deteriorated at times, but substantial improvements are noted in the higher resolution simulation. The representation of extreme precipitation events in summer and the simulation of winter temperature are better represented in the convection-permitting simulation. Furthermore, the observed temperature–extreme precipitation scaling is realistically reproduced by the higher resolution simulation. The use of convective-permitting resolution simulations to study the wind and the PBL in the Arctic can produce results that will be able to support climate impact assessment studies such as those related to engineering applications and where high spatial and temporal resolutions are beneficial.

In addition to model improvements, new diagnostics can be developed such as machine learning-based approaches to support detailed analysis. For example, applying clustering analysis to wind profiles, separating distinct categories of wind profiles based on the stability regime, would be useful as each regime has a specific wind distribution with a different potential for energy production.

The planetary boundary layer in the Arctic has two preferred states, one where the surface and atmosphere are in radiative-turbulent near-equilibrium characterized by higher wind speed, low-level clouds with high cloud water content and shallow and weak temperature inversions (weakly stable boundary layer – WSBL), and a cold and radiatively clear state with lower wind speed, lower percentage of cloud fraction, intense radiative cooling and strong temperature inversions (very stable boundary layer – VSBL). In a future warmer climate, the frequency of the WSBL regime will increase, leading to fewer and weaker temperature inversions, and higher wind speed, leading to a scenario more favorable for wind as a resource.

The temperature inversion strength defined in chapter 3 can be used to characterize the stability condition of the planetary boundary layer before using a machine learning clustering analysis technique to further classify each stability regime. Using this technique, useful information can be created, such as the prevalence of each regime and the altitude where the maximum wind speed is present for each regime.

Figure 11 shows some preliminary results using a machine learning clustering analysis technique, based on the work of Sommerfeld et al. (2019) to categorize the vertical profile of wind at selected sites in Arctic Canada, dividing it between four planetary boundary layer stability regimes. The vertical profiles were first divided by the sign of the temperature inversion strength (ΔT), where negative values indicate unstable regimes, and positive ones indicate stable regimes. K-mean clustering analysis was applied to each group, to further differentiate it into four regimes: unstable and shear driven for the unstable PBL and weakly stable boundary layer (WSBL) and very stable boundary layer (VSBL) for the stable PBL. This analysis was done using the atmospheric soundings and model data from the GEM-ERA simulation for the current climate, using the 1986-2015 period to assess the model capability of representing the wind profiles.

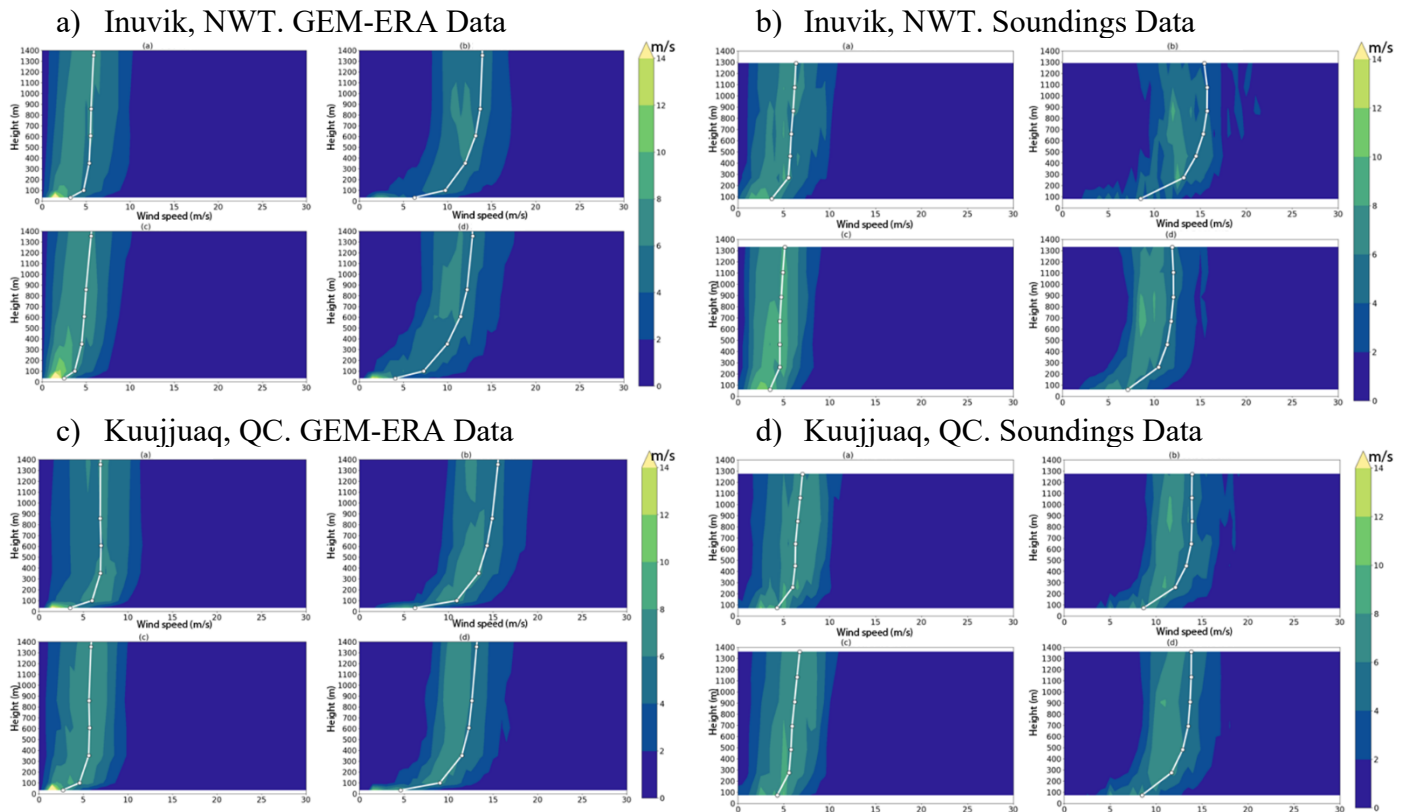


Figure 11: Vertical profiles of the mean wind speed (in m/s) for two locations in Arctic Canada: Inuvik and Kuujjuaq, for the DJF period of 1986-2015. Colors indicate the percentage of each wind speed, and each altitude sums up to 100%. The white line plot indicates the centroids of the k-mean clustering analysis. Each subplot has 4 small plots, separated by the temperature inversion strength (ΔT) and

stability regime, top left subplot: ΔT^+ , VSBL; top right: ΔT^+ , WSBL; bottom left: ΔT^- , unstable; bottom right: ΔT^- , shear driven.

Positive values of ΔT indicate the presence of temperature inversions. Although the soundings only have twice-daily data (0 and 12Z) and the model has 3 hourly data, the percentage of each PBL regime into their subcategory are similar, as are the wind speed values. The results show that unstable or stable regimes have two different sub-regimes with different wind speed profiles, leading to distinct optimal height and mean wind energy generation. The percentage of the regimes with maximum wind energy generation is low, but they are posed to generate much more wind energy due to having almost double mean wind speed. Similar analysis can be extended to transient climate change simulations, to see which regime will be more prevalent in a warmer climate, and how it can affect the wind as a resource in the near future.

REFERENCES

- Abraham, C., & Monahan, A. H. (2019). Climatological features of the weakly and very stably stratified nocturnal boundary layers. Part II: Regime occupation and transition statistics and the influence of external drivers. *Journal of the Atmospheric Sciences*, 76(11), 3485–3504. <https://doi.org/10.1175/JAS-D-19-0078.1>
- AIRS project. (2019). Aqua/AIRS L3 Daily Standard Physical Retrieval (AIRS+AMSU) 1 degree x 1 degree V7.0, Greenbelt, MD, USA, Goddard Earth Sciences Data and Information Services Center (GES DISC). <https://doi.org/10.5067/8XB4RU470FJV>
- Alexander, M. A., Tomas, R., Deser, C., & Lawrence, D. M. (2010). The atmospheric response to projected terrestrial snow changes in the late twenty-first century. *Journal of Climate*, 23(23), 6430–6437. <https://doi.org/10.1175/2010JCLI3899.1>
- Alsaleh, A., & Sattler, M. (2019). Life cycle assessment of large wind turbines in the US: A Texas case study. In *Proceedings of the Air and Waste Management Association's Annual Conference and Exhibition, AWMA* (Vol. 2019-June, pp. 887–903). Springer Verlag. <https://doi.org/10.1007/S10098-019-01678-0/TABLES/18>
- Bélair, S., Mailhot, J., Girard, C., & Vaillancourt, P. (2005). Boundary layer and shallow cumulus clouds in a medium-range forecast of a large-scale weather system. *Monthly Weather Review*, 133(7), 1938–1960. <https://doi.org/10.1175/MWR2958.1>
- Benoit, R., Côté, J., & Mailhot, J. (1989). Inclusion of a TKE Boundary Layer Parameterization in the Canadian Regional Finite-Element Model. *Monthly Weather Review*, 117(8), 1726–1750. [https://doi.org/10.1175/1520-0493\(1989\)117<1726:Ioatbl>2.0.Co;2](https://doi.org/10.1175/1520-0493(1989)117<1726:Ioatbl>2.0.Co;2)
- Berrisford, P., Dee, D., Poli, P., Brugge, R., Fielding, K., Fuentes, M., ... Simmons, A. (2009). *The ERA-Interim Archive Version 2.0. ERA report series* (Vol. 1). Shinfield Park, Reading: ECMWF. Retrieved from <http://www.ecmwf.int/publications/library/do/references/list/782009>
- Bintanja, R., & Andry, O. (2017). Towards a rain-dominated Arctic. *Nature Climate Change*, 7(4), 263–267. <https://doi.org/10.1038/nclimate3240>
- Bintanja, R., Graverson, R. G., & Hazeleger, W. (2011). Arctic winter warming amplified by the thermal inversion and consequent low infrared cooling to space. *Nature Geoscience*, 4(11), 758–761. <https://doi.org/10.1038/ngeo1285>
- Boé, J., Hall, A., & Qu, X. (2009, September 1). Current GCMs' Unrealistic Negative Feedback in the Arctic. *Journal of Climate*. <https://doi.org/10.1175/2009JCLI2885.1>
- Boisvert, L. N., & Stroeve, J. C. (2015). The Arctic is becoming warmer and wetter as revealed by the Atmospheric Infrared Sounder. *Geophysical Research Letters*, 42(11), 4439–4446. <https://doi.org/10.1002/2015GL063775>
- Bracegirdle, T. J., & Stephenson, D. B. (2013). On the robustness of emergent constraints used in multimodel climate change projections of arctic warming. *Journal of Climate*, 26(2), 669–678. <https://doi.org/10.1175/JCLI-D-12-00537.1>
- Bradley, R. S., Keimig, F. T., & Diaz, H. F. (1992). Climatology of surface-based inversions in the North American Arctic. *Journal of Geophysical Research*, 97(D14), 15699–15712. <https://doi.org/10.1029/92jd01451>
- Cairns, S., & Mccarney, G. (2021). Solar and Wind Energy in Canada: Value Recovery and End-of-life Considerations | *Smart Prosperity Institute*.
- Canada, C.-I. R. and N. A. (2020). The Northern Abandoned Mine Reclamation Program Backgrounder, 1–8. Retrieved from <https://www.canada.ca/en/crown-indigenous-relations-northern-affairs/news/2019/08/the-northern-abandoned-mine-reclamation-program.html>
- CanREA. (2021). Sustainable Energy: Recycling Renewables. *Canadian Renewable Energy Association*. Retrieved from www.renewablesassociation.ca

- CBC news. (2018). How will wind power change Inuvik? N.W.T. energy director gives the details. Retrieved from <https://www.cbc.ca/news/canada/north/wind-power-andrew-stewart-q-and-a-1.4907876>
- Cerrai, D., Koukoulou, M., Watson, P., & Anagnostou, E. N. (2020). Outage prediction models for snow and ice storms. *Sustainable Energy, Grids and Networks*, *21*, 100294. <https://doi.org/10.1016/j.segan.2019.100294>
- Chang, L., Feng, G., Zhang, Y., & He, X. (2018). Effect of cloud fraction on arctic low-level temperature inversions in AIRS observations over both land and ocean. *IEEE Transactions on Geoscience and Remote Sensing*, *56*(4), 2025–2032. <https://doi.org/10.1109/TGRS.2017.2772297>
- Chang, L., Wen, S., Gao, G., Han, Z., Feng, G., & Zhang, Y. (2021). Assessment of temperature and specific humidity inversions and their relationships in three global reanalysis products over the arctic ocean. *Journal of Applied Meteorology and Climatology*, *60*(4), 493–511. <https://doi.org/10.1175/JAMC-D-20-0079.1>
- Cholette, M., Laprise, R., & Thériault, J. (2015). Perspectives for Very High-Resolution Climate Simulations with Nested Models: Illustration of Potential in Simulating St. Lawrence River Valley Channelling Winds with the Fifth-Generation Canadian Regional Climate Model. *Climate*, *3*(2), 283–307. <https://doi.org/10.3390/cli3020283>
- Chylek, P., Li, J., Dubey, M. K., Wang, M., & Lesins, G. (2011). Observed and model simulated 20th century Arctic temperature variability: Canadian Earth System Model CanESM2. *Atmospheric Chemistry and Physics Discussions*, *11*(8), 22893–22907. <https://doi.org/10.5194/acpd-11-22893-2011>
- Cohen, J., Screen, J. A., Furtado, J. C., Barlow, M., Whittleston, D., Coumou, D., ... Jones, J. (2014). Recent Arctic amplification and extreme mid-latitude weather. *Nature Geoscience*, *7*(9), 627. <https://doi.org/10.1038/ngeo2234>
- Côté, J., Gravel, S., Méthot, A., Patoine, A., Roch, M., & Staniforth, A. (1998). The operational CMC-MRB global environmental multiscale (GEM) model. Part I: Design considerations and formulation. *Monthly Weather Review*, *126*(6), 1373–1395. [https://doi.org/10.1175/1520-0493\(1998\)126<1373:TOCMGE>2.0.CO;2](https://doi.org/10.1175/1520-0493(1998)126<1373:TOCMGE>2.0.CO;2)
- Coumou, D., Di Capua, G., Vavrus, S., Wang, L., & Wang, S. (2018). The influence of Arctic amplification on mid-latitude summer circulation. *Nature Communications*. <https://doi.org/10.1038/s41467-018-05256-8>
- Daines, J. T., Monahan, A. H., & Curry, C. L. (2016). Model-based projections and uncertainties of near-surface wind climate in western Canada. *Journal of Applied Meteorology and Climatology*, *55*(10), 2229–2245. <https://doi.org/10.1175/JAMC-D-16-0091.1>
- Davenport, F. V., & Diffenbaugh, N. S. (2021). Using Machine Learning to Analyze Physical Causes of Climate Change: A Case Study of U.S. Midwest Extreme Precipitation. *Geophysical Research Letters*, *48*(15), e2021GL093787. <https://doi.org/10.1029/2021GL093787>
- Dee, D. P., Uppala, S. M., Simmons, A. J., Berrisford, P., Poli, P., Kobayashi, S., ... Vitart, F. (2011). The ERA-Interim reanalysis: Configuration and performance of the data assimilation system. *Quarterly Journal of the Royal Meteorological Society*, *137*(656), 553–597. <https://doi.org/10.1002/qj.828>
- Delage, Y. (1997). Parameterising sub-grid scale vertical transport in atmospheric models under statically stable conditions. *Boundary-Layer Meteorology*, *82*(1), 23–48. <https://doi.org/10.1023/a:1000132524077>
- Delage, Y., & Girard, C. (1992). Stability functions correct at the free convection limit and consistent for for both the surface and Ekman layers. *Boundary-Layer Meteorology*, *58*(1), 19–31. <https://doi.org/10.1007/bf00120749>
- Deser, C., Tomas, R., Alexander, M., & Lawrence, D. (2010). The seasonal atmospheric response to projected Arctic sea ice loss in the late twenty-first century. *Journal of Climate*, *23*(2), 333–351. <https://doi.org/10.1175/2009JCLI3053.1>
- Devasthale, A., Willén, U., Karlsson, K. G., & Jones, C. G. (2010). Quantifying the clear-sky temperature inversion frequency and strength over the Arctic Ocean during summer and winter seasons from AIRS profiles. *Atmospheric Chemistry and Physics*, *10*(12), 5565–5572. <https://doi.org/10.5194/acp-10-5565-2010>
- Diro, G. T., & Sushama, L. (2017). The role of soil moisture-atmosphere interaction on future hot spells over

- North America as simulated by the Canadian Regional Climate Model (CRCM5). *Journal of Climate*, 30(13), 5041–5058. <https://doi.org/10.1175/JCLI-D-16-0068.1>
- Diro, G. T., & Sushama, L. (2019). Simulating Canadian Arctic Climate at Convection-Permitting Resolution. *Atmosphere*, 10(8), 430. <https://doi.org/10.3390/atmos10080430>
- Diro, G. T., Sushama, L., Martynov, A., Jeong, D. I., Verseghy, D., & Winger, K. (2014). Land-atmosphere coupling over North America in CRCM5. *Journal of Geophysical Research*, 119(21), 11,955–11,972. <https://doi.org/10.1002/2014JD021677>
- Dörenkämper, M., Optis, M., Monahan, A., & Steinfeld, G. (2015). On the Offshore Advection of Boundary-Layer Structures and the Influence on Offshore Wind Conditions. *Boundary-Layer Meteorology*, 155(3), 459–482. <https://doi.org/10.1007/s10546-015-0008-x>
- Dukhan, T., & Sushama, L. (2021). Understanding and modelling future wind-driven rain loads on building envelopes for Canada. *Building and Environment*, 196, 107800. <https://doi.org/10.1016/j.buildenv.2021.107800>
- Durre, I., Vose, R. S., & Wuertz, D. B. (2006). Overview of the integrated global radiosonde archive. *Journal of Climate*, 19(1), 53–68. <https://doi.org/10.1175/JCLI3594.1>
- ecoENERGY Innovation Initiative. (2016). *Glencore RAGLAN Mine Renewable Electricity Smart-Grid Pilot Demonstration*.
- Farchi, A., Laloyaux, P., Bonavita, M., & Bocquet, M. (2021). Using machine learning to correct model error in data assimilation and forecast applications. *Quarterly Journal of the Royal Meteorological Society*, 147(739), 3067–3084. <https://doi.org/10.1002/qj.4116>
- Fernando, H. J. S., & Weil, J. C. (2010). Whither the stable boundary layer? *Bulletin of the American Meteorological Society*, 91(11), 1475–1484. <https://doi.org/10.1175/2010BAMS2770.1>
- Feser, F., Rrockel, B., Storch, H., Winterfeldt, J., & Zahn, M. (2011). Regional climate models add value to global model data a review and selected examples. *Bulletin of the American Meteorological Society*, 92(9), 1181–1192. <https://doi.org/10.1175/2011BAMS3061.1>
- Fochesatto, G. J. (2015). Methodology for determining multilayered temperature inversions. *Atmospheric Measurement Techniques*, 8(5), 2051–2060. <https://doi.org/10.5194/amt-8-2051-2015>
- Foley, A. M. (2010). Uncertainty in regional climate modelling: A review. *Progress in Physical Geography*, 34(5), 647–670. <https://doi.org/10.1177/0309133310375654>
- Generation Energy. (2018). *Canada's Energy Transition: Getting to Our Energy Future, Together*.
- Gillett, N. P., Stone, D. A., Stott, P. A., Nozawa, T., Karpechko, A. Y., Hegerl, G. C., ... Jones, P. D. (2008). Attribution of polar warming to human influence. *Nature Geoscience*, 1, 750. Retrieved from <https://doi.org/10.1038/ngeo338>
- Harris, I., Jones, P. D., Osborn, T. J., & Lister, D. H. (2014). Updated high-resolution grids of monthly climatic observations - the CRU TS3.10 Dataset. *International Journal of Climatology*, 34(3), 623–642. <https://doi.org/10.1002/joc.3711>
- He, Y., Monahan, A. H., Jones, C. G., Dai, A., Biner, S., Caya, D., & Winger, K. (2010). Probability distributions of land surface wind speeds over North America. *Journal of Geophysical Research Atmospheres*, 115(4), D04103. <https://doi.org/10.1029/2008JD010708>
- He, Y., Monahan, A. H., & McFarlane, N. A. (2013). Diurnal variations of land surface wind speed probability distributions under clear-sky and low-cloud conditions. *Geophysical Research Letters*, 40(12), 3308–3314. <https://doi.org/10.1002/grl.50575>
- Hearty, T. J., Savtchenko, A., Tian, B., Fetzer, E., Yung, Y. L., Theobald, M., ... Won, Y. I. (2014). Estimating sampling biases and measurement uncertainties of AIRS/AMSU-A temperature and water vapor observations using MERRA reanalysis. *Journal of Geophysical Research*, 119(6), 2725–2741.

<https://doi.org/10.1002/2013JD021205>

- Hernández-Díaz, L., Laprise, R., Sushama, L., Martynov, A., Winger, K., & Dugas, B. (2013). Climate simulation over CORDEX Africa domain using the fifth-generation Canadian Regional Climate Model (CRCM5). *Climate Dynamics*, *40*(5–6), 1415–1433. <https://doi.org/10.1007/s00382-012-1387-z>
- Hohenegger, C., Brockhaus, P., Bretherton, C. S., & Schär, C. (2009). The soil moisture-precipitation feedback in simulations with explicit and parameterized convection. *Journal of Climate*, *22*(19), 5003–5020. <https://doi.org/10.1175/2009JCLI2604.1>
- Holland, M. M., & Bitz, C. M. (2003). Polar amplification of climate change in coupled models. *Climate Dynamics*, *21*(3–4), 221–232. <https://doi.org/10.1007/s00382-003-0332-6>
- Holtslag, A. A. M., Svensson, G., Baas, P., Basu, S., Beare, B., Beljaars, A. C. M., ... Van De Wiel, B. J. H. (2013). Stable atmospheric boundary layers and diurnal cycles: Challenges for weather and climate models. *Bulletin of the American Meteorological Society*, *94*(11), 1691–1706. <https://doi.org/10.1175/BAMS-D-11-00187.1>
- Hwang, Y. T., Frierson, D. M. W., & Kay, J. E. (2011). Coupling between Arctic feedbacks and changes in poleward energy transport. *Geophysical Research Letters*, *38*(17), n/a-n/a. <https://doi.org/10.1029/2011GL048546>
- Infrastructure Canada. (2019). Inuvik Wind Generation. Retrieved July 15, 2019, from <https://www.infrastructure.gc.ca/investments-2002-investissements/projects-list-liste-de-projets-eng.html?pt=nt&cat=Green Energy>
- IPCC. (2013). *Climate Change 2013 - The Physical Science Basis. Climate Change 2013 - The Physical Science Basis*. <https://doi.org/10.1017/cbo9781107415324>
- Jensen, J. P. (2019). Evaluating the environmental impacts of recycling wind turbines. *Wind Energy*, *22*(2), 316–326. <https://doi.org/10.1002/we.2287>
- Jeong, D. Il, & Sushama, L. (2017). Projected changes to surface wind characteristics and extremes over North America in CRCM5. *19th EGU General Assembly, EGU2017, Proceedings from the Conference Held 23-28 April, 2017 in Vienna, Austria., p.225, 19, 225*. Retrieved from <http://adsabs.harvard.edu/abs/2017EGUGA..19..225J>
- Jeong, D. Il, & Sushama, L. (2018). Projected changes to extreme wind and snow environmental loads for buildings and infrastructure across Canada. *Sustainable Cities and Society*, *36*, 225–236. <https://doi.org/10.1016/j.scs.2017.10.004>
- Kahl, J. D. (1990). Characteristics of the low-level temperature inversion along the Alaskan Arctic coast. *International Journal of Climatology*, *10*(5), 537–548. <https://doi.org/10.1002/joc.3370100509>
- Kain, J. S., & Fritsch, J. M. (1990). A one-dimensional entraining/detraining plume model and its application in convective parameterization. *Journal of the Atmospheric Sciences*, *47*(23), 2784–2802. [https://doi.org/10.1175/1520-0469\(1990\)047<2784:AODEPM>2.0.CO;2](https://doi.org/10.1175/1520-0469(1990)047<2784:AODEPM>2.0.CO;2)
- Kendon, E. J., Ban, N., Roberts, N. M., Fowler, H. J., Roberts, M. J., Chan, S. C., ... Wilkinson, J. M. (2017). Do convection-permitting regional climate models improve projections of future precipitation change? *Bulletin of the American Meteorological Society*, *98*(1), 79–93. <https://doi.org/10.1175/BAMS-D-15-0004.1>
- Knowles, J. (2016). Power Shift: Electricity for Canada’s Remote Communities.
- Koenigk, T., Key, J., & Vihma, T. (2020). Climate Change in the Arctic (pp. 673–705). Springer, Cham. https://doi.org/10.1007/978-3-030-33566-3_11
- Kumar, I., Tyner, W. E., & Sinha, K. C. (2016). Input-output life cycle environmental assessment of greenhouse gas emissions from utility scale wind energy in the United States. *Energy Policy*, *89*(C), 294–301. <https://doi.org/10.1016/j.enpol.2015.12.004>
- Kuo, H. L. (1965). On Formation and Intensification of Tropical Cyclones Through Latent Heat Release by

- Cumulus Convection. *Journal of the Atmospheric Sciences*, 22(1), 40–63. [https://doi.org/10.1175/1520-0469\(1965\)022<0040:ofaiot>2.0.co;2](https://doi.org/10.1175/1520-0469(1965)022<0040:ofaiot>2.0.co;2)
- Laprise, R. (2008). Regional climate modelling. *Journal of Computational Physics*, 227(7), 3641–3666. <https://doi.org/10.1016/j.jcp.2006.10.024>
- Lawrence, D. M., Slater, A. G., Tomas, R. A., Holland, M. M., & Deser, C. (2008). Accelerated Arctic land warming and permafrost degradation during rapid sea ice loss. *Geophysical Research Letters*, 35(11), L11506. <https://doi.org/10.1029/2008GL033985>
- Leduc, M., & Laprise, R. (2009). Regional climate model sensitivity to domain size. *Climate Dynamics*, 32(6), 833–854. <https://doi.org/10.1007/s00382-008-0400-z>
- Li, J., & Barker, H. W. (2005). A radiation algorithm with correlated-k distribution. Part I: Local thermal equilibrium. *Journal of the Atmospheric Sciences*, 62(2), 286–309. <https://doi.org/10.1175/JAS-3396.1>
- Lindsay, R., Wensnahan, M., Schweiger, A., & Zhang, J. (2014). Evaluation of seven different atmospheric reanalysis products in the arctic. *Journal of Climate*, 27(7), 2588–2606. <https://doi.org/10.1175/JCLI-D-13-00014.1>
- Liu, J., Zhang, Z., Hu, Y. Y., Chen, L., Dai, Y., & Ren, X. (2008). Assessment of surface air temperature over the Arctic Ocean in reanalysis and IPCC AR4 model simulations with IABP/POLES observations. *Journal of Geophysical Research Atmospheres*, 113(10), D10105. <https://doi.org/10.1029/2007JD009380>
- Liu, Y., Key, J. R., Schweiger, A., & Francis, J. (2006). Characteristics of satellite-derived clear-sky atmospheric temperature inversion strength in the Arctic, 1980–96. *Journal of Climate*, 19(19), 4902–4913. <https://doi.org/10.1175/JCLI3915.1>
- Mahlstein, I., & Knutti, R. (2011). Ocean heat transport as a cause for model uncertainty in projected arctic warming. *Journal of Climate*, 24(5), 1451–1460. <https://doi.org/10.1175/2010JCLI3713.1>
- Mahrt, L. (1998). Stratified atmospheric boundary layers and breakdown of models. *Theoretical and Computational Fluid Dynamics*, 11(3–4), 263–279. <https://doi.org/10.1007/s001620050093>
- Manabe, S., & Stouffer, R. J. (1980). Sensitivity of a global climate model to an increase of CO₂ concentration in the atmosphere. *Journal of Geophysical Research*, 85(C10), 5529–5554. <https://doi.org/10.1029/JC085iC10p05529>
- Martynov, A., Laprise, R., Sushama, L., Winger, K., Šeparović, L., & Dugas, B. (2013). Reanalysis-driven climate simulation over CORDEX North America domain using the Canadian Regional Climate Model, version 5: Model performance evaluation. *Climate Dynamics*, 41(11–12), 2973–3005. <https://doi.org/10.1007/s00382-013-1778-9>
- Matangi, A. (2014). *Wind resource assessment Storm Hills, NWT*. Retrieved from https://nwtresearch.com/sites/default/files/2014-06-11_storm_hills_nwt_wra.pdf
- Matthes, H., Rinke, A., Miller, P. A., Kuhry, P., Dethloff, K., & Wolf, A. (2012). Sensitivity of high-resolution Arctic regional climate model projections to different implementations of land surface processes. *Climatic Change*, 111(2), 197–214. <https://doi.org/10.1007/s10584-011-0138-1>
- Matthes, H., Rinke, A., Zhou, X., & Dethloff, K. (2017). Uncertainties in coupled regional Arctic climate simulations associated with the used land surface model. *Journal of Geophysical Research*, 122(15), 7755–7771. <https://doi.org/10.1002/2016JD026213>
- Mauritsen, T., & Svensson, G. (2007). Observations of Stably Stratified Shear-Driven Atmospheric Turbulence at Low and High Richardson Numbers. *Journal of the Atmospheric Sciences*, 64(2), 645–655. <https://doi.org/10.1175/jas3856.1>
- Mayfield, J. A., Fochesatto, G. J., Mayfield, J. A., & Fochesatto, G. J. (2013). The Layered Structure of the Winter Atmospheric Boundary Layer in the Interior of Alaska. *Journal of Applied Meteorology and Climatology*, 52(4), 953–973. <https://doi.org/10.1175/JAMC-D-12-01.1>

- McFarlane, N. A. (1987). The Effect of Orographically Excited Gravity Wave Drag on the General Circulation of the Lower Stratosphere and Troposphere. *Journal of the Atmospheric Sciences*, 44(14), 1775–1800. [https://doi.org/10.1175/1520-0469\(1987\)044<1775:teooeg>2.0.co;2](https://doi.org/10.1175/1520-0469(1987)044<1775:teooeg>2.0.co;2)
- McInnes, K. L., Erwin, T. A., & Bathols, J. M. (2011). Global Climate Model projected changes in 10 m wind speed and direction due to anthropogenic climate change. *Atmospheric Science Letters*, 12(4), 325–333. <https://doi.org/10.1002/asl.341>
- Medeiros, B., Deser, C., Tomas, R. A., & Kay, J. E. (2011). Arctic inversion strength in climate models. *Journal of Climate*, 24(17), 4733–4740. <https://doi.org/10.1175/2011JCLI3968.1>
- Mironov, D., Rontu, L., Kourzeneva, E., & Terzhevik, A. (2010). Towards improved representation of lakes in numerical weather prediction and climate models: Introduction to the special issue of Boreal Environment Research. *Boreal Environment Research*, 15(97–99).
- Monahan, A. H., Rees, T., He, Y., McFarlane, N., Monahan, A. H., Rees, T., ... McFarlane, N. (2015). Multiple Regimes of Wind, Stratification, and Turbulence in the Stable Boundary Layer. *Journal of the Atmospheric Sciences*, 72(8), 3178–3198. <https://doi.org/10.1175/JAS-D-14-0311.1>
- Morrison, A. L., Kay, J. E., Frey, W. R., Chepfer, H., & Guzman, R. (2019). Cloud Response to Arctic Sea Ice Loss and Implications for Future Feedback in the CESM1 Climate Model. *Journal of Geophysical Research: Atmospheres*, 124(2), 1003–1020. <https://doi.org/10.1029/2018JD029142>
- Natural Resources Canada. (2020). Permafrost thaw brings major problems to Canada's Northern Arctic communities. Retrieved December 10, 2021, from <https://www.nrcan.gc.ca/simply-science/permafrost-thaw-brings-major-problems-canadas-northern-arctic-communities/23233>
- Oh, S.-G., & Sushama, L. (2020). Short-duration precipitation extremes over Canada in a warmer climate. *Climate Dynamics*, 54(3), 2493–2509. <https://doi.org/10.1007/s00382-020-05126-4>
- Overland, J., Dunlea, E., Box, J. E., Corell, R., Forsius, M., Kattsov, V., ... Wang, M. (2019). The urgency of Arctic change. *Polar Science*. Elsevier B.V. <https://doi.org/10.1016/j.polar.2018.11.008>
- Palo, T., Vihma, T., Jaagus, J., & Jakobson, E. (2017). Observations of temperature inversions over central Arctic sea ice in summer. *Quarterly Journal of the Royal Meteorological Society*, 143(708), 2741–2754. <https://doi.org/10.1002/qj.3123>
- Pavelsky, T. M., Boé, J., Hall, A., & Fetzer, E. J. (2011). Atmospheric inversion strength over polar oceans in winter regulated by sea ice. *Climate Dynamics*, 36(5–6), 945–955. <https://doi.org/10.1007/s00382-010-0756-8>
- Pinard, J. (2016). *Inuvik Wind Monitoring Update 2016*. Retrieved from http://nwtresearch.com/sites/default/files/inuvik_wind_monitoring_update_2016.pdf
- Prein, A. F., Langhans, W., Fossier, G., Ferrone, A., Ban, N., Goergen, K., ... Leung, R. (2015). A review on regional convection-permitting climate modeling: Demonstrations, prospects, and challenges. *Reviews of Geophysics*, 53(2), 323–361. <https://doi.org/10.1002/2014RG000475>
- Riahi, K., Rao, S., Krey, V., Cho, C., Chirkov, V., Fischer, G., ... Rafaj, P. (2011). RCP 8.5-A scenario of comparatively high greenhouse gas emissions. *Climatic Change*, 109(1), 33–57. <https://doi.org/10.1007/s10584-011-0149-y>
- Richards, G., Noble, B., & Belcher, K. (2012). Barriers to renewable energy development: A case study of large-scale wind energy in Saskatchewan, Canada. *Energy Policy*, 42, 691–698. <https://doi.org/10.1016/j.enpol.2011.12.049>
- Roeckner, E., Brokopf, R., Esch, M., Giorgetta, M., Hagemann, S., Kornbluh, L., ... Schulzweida, U. (2006). Sensitivity of Simulated Climate to Horizontal and Vertical Resolution in the ECHAM5 Atmosphere Model. *Journal of Climate*, 19(16), 3771–3791. <https://doi.org/10.1175/JCLI3824.1>
- Rowell, D. P. (2012). Sources of uncertainty in future changes in local precipitation. *Climate Dynamics*, 39(7–8), 1929–1950. <https://doi.org/10.1007/s00382-011-1210-2>

- Rummukainen, M. (2010). State-of-the-art with regional climate models. *Wiley Interdisciplinary Reviews: Climate Change*, 1(1), 82–96. <https://doi.org/10.1002/wcc.8>
- Schreiber, M. (2018). Melting Permafrost and the Housing Crisis in the Arctic. *Bloomberg*. Retrieved from <https://www.bloomberg.com/news/articles/2018-05-10/melting-permafrost-and-the-housing-crisis-in-the-arctic>
- Screen, J. A., & Simmonds, I. (2010a). Increasing fall-winter energy loss from the Arctic Ocean and its role in Arctic temperature amplification. *Geophysical Research Letters*, 37(16), n/a-n/a. <https://doi.org/10.1029/2010GL044136>
- Screen, J. A., & Simmonds, I. (2010b). The central role of diminishing sea ice in recent Arctic temperature amplification. *Nature*, 464(7293), 1334–1337. <https://doi.org/10.1038/nature09051>
- Šeparović, L., Alexandru, A., Laprise, R., Martynov, A., Sushama, L., Winger, K., ... Valin, M. (2013). Present climate and climate change over North America as simulated by the fifth-generation Canadian regional climate model. *Climate Dynamics*, 41(11–12), 3167–3201. <https://doi.org/10.1007/s00382-013-1737-5>
- Serreze, M. C., Barrett, A. P., Stroeve, J. C., Kindig, D. N., & Holland, M. M. (2009). The emergence of surface-based Arctic amplification. *Cryosphere*, 3(1), 11–19. <https://doi.org/10.5194/tc-3-11-2009>
- Serreze, Mark C., & Barry, R. G. (2006). The Arctic climate system. *Choice Reviews Online*, 44(01), 44-0373-44-0373. <https://doi.org/10.5860/choice.44-0373>
- Sommerfeld, M., Crawford, C., Monahan, A., & Bastigkeit, I. (2019). LiDAR-based characterization of mid-altitude wind conditions for airborne wind energy systems. *Wind Energy*, we.2343. <https://doi.org/10.1002/we.2343>
- Sundqvist, H., Berge, E., & Kristjansson, J. E. (1989). Condensation and cloud parameterization studies with a mesoscale numerical weather prediction model. *Monthly Weather Review*, 117(8), 1641–1657. [https://doi.org/10.1175/1520-0493\(1989\)117<1641:CACPSW>2.0.CO;2](https://doi.org/10.1175/1520-0493(1989)117<1641:CACPSW>2.0.CO;2)
- Teufel, B., & Sushama, L. (2019). Abrupt changes across the Arctic permafrost region endanger northern development. *Nature Climate Change*. Nature Publishing Group. <https://doi.org/10.1038/s41558-019-0614-6>
- Teufel, Bernardo, Sushama, L., Arora, V. K., & Versegny, D. (2019). Impact of dynamic vegetation phenology on the simulated pan-Arctic land surface state. *Climate Dynamics*, 52(1–2), 373–388. <https://doi.org/10.1007/s00382-018-4142-2>
- The Northern Miner. (2021). Feds announce \$7.1M for new wind turbines at Raglan mine - The Northern Miner. Retrieved December 10, 2021, from <https://www.northernminer.com/news/feds-announce-7-1m-for-new-wind-turbines-at-raglan-mine/1003829126/>
- Tian, B., Fetzer, E. J., Kahn, B. H., Teixeira, J., Manning, E., & Hearty, T. (2013). Evaluating CMIP5 models using AIRS tropospheric air temperature and specific humidity climatology. *Journal of Geophysical Research Atmospheres*, 118(1), 114–134. <https://doi.org/10.1029/2012JD018607>
- Tjernström, M., Shupe, M. D., Brooks, I. M., Achtert, P., Prytherch, J., & Sedlar, J. (2019). Arctic summer airmass transformation, surface inversions, and the surface energy budget. *Journal of Climate*, 32(3), 769–789. <https://doi.org/10.1175/JCLI-D-18-0216.1>
- Van de Wiel, B. J. H., Vignon, E., Baas, P., van Hooijdonk, I. G. S., van der Linden, S. J. A., van Hooft, J. A., ... Genthon, C. (2017). Regime transitions in near-surface temperature inversions: A conceptual model. *Journal of the Atmospheric Sciences*, 74(4), 1057–1073. <https://doi.org/10.1175/JAS-D-16-0180.1>
- van Vuuren, D. P., Edmonds, J., Kainuma, M., Riahi, K., Thomson, A., Hibbard, K., ... Rose, S. K. (2011). The representative concentration pathways: An overview. *Climatic Change*, 109(1), 5–31. <https://doi.org/10.1007/s10584-011-0148-z>
- Versegny, D. (2009). CLASS - The Canadian Land Surface Scheme (Version 3.4), Technical Documentation (Version 1.1). *Climate Research Division, Science and Technology Branch, Downsview, Ontario, Canada*,

(January), 180.

- Verseghy, D. L., McFarlane, N. A., & Lazare, M. (1993). CLASS - A Canadian land surface scheme for GCMS, II. Vegetation model and coupled runs. *International Journal of Climatology*, 13(4), 347–370. <https://doi.org/10.1002/joc.3370130402>
- Verseghy, Diana L. (1991). CLASS - A Canadian land surface scheme for GCMS. I. Soil model. *International Journal of Climatology*, 11(2), 111–133. <https://doi.org/10.1002/joc.3370110202>
- Wang, D., Guo, J., Chen, A., Bian, L., Ding, M., Liu, L., ... Han, Y. (2020). Temperature Inversion and Clouds Over the Arctic Ocean Observed by the 5th Chinese National Arctic Research Expedition. *Journal of Geophysical Research: Atmospheres*, 125(13), e2019JD032136. <https://doi.org/10.1029/2019JD032136>
- Werner, A. T. (2011). *BCSD Downscaled Transient Climate Projections for Eight Select GCMs over British Columbia, Canada*. Pacific Climate Impacts Consortium. Retrieved from <http://citeserx.ist.psu.edu/viewdoc/download?doi=10.1.1.438.7992&rep=rep1&type=pdf>
- Wetzel, C., & Brümmer, B. (2011). An Arctic inversion climatology based on the European Centre Reanalysis ERA-40. *Meteorologische Zeitschrift*, 20(6), 589–600. <https://doi.org/10.1127/0941-2948/2011/0295>
- Yeh, K. S., Côté, J., Gravel, S., Méthot, A., Patoine, A., Roch, M., & Staniforth, A. (2002). The CMC-MRB Global Environmental Multiscale (GEM) model. Part III: Nonhydrostatic formulation. *Monthly Weather Review*, 130(2), 339–356. [https://doi.org/10.1175/1520-0493\(2002\)130<0339:TCMGEM>2.0.CO;2](https://doi.org/10.1175/1520-0493(2002)130<0339:TCMGEM>2.0.CO;2)
- Yuval, J., & O’Gorman, P. A. (2020). Stable machine-learning parameterization of subgrid processes for climate modeling at a range of resolutions. *Nature Communications* 2020 11:1, 11(1), 1–10. <https://doi.org/10.1038/s41467-020-17142-3>
- Zadra, A., Roch, M., Laroche, S., & Charron, M. (2003). The subgrid-scale orographic blocking parametrization of the GEM Model. *Atmosphere-Ocean*, 41(2), 155–170. <https://doi.org/10.3137/ao.410204>
- Zhang, Lei, Li, J., Ding, M., Guo, J., Bian, L., Sun, Q., ... Zhang, D. (2021). Characteristics of low-level temperature inversions over the Arctic Ocean during the CHINARE 2018 campaign in summer. *Atmospheric Environment*, 253, 118333. <https://doi.org/10.1016/j.atmosenv.2021.118333>
- Zhang, Lin, Ding, M., Dou, T., Huang, Y., Lv, J., & Xiao, C. (2021). The shallowing surface temperature inversions in the arctic. *Journal of Climate*, 34(10), 4159–4168. <https://doi.org/10.1175/JCLI-D-20-0621.1>
- Zhang, Y., & Seidel, D. J. (2011). Challenges in estimating trends in Arctic surface-based inversions from radiosonde data. *Geophysical Research Letters*, 38(17), n/a-n/a. <https://doi.org/10.1029/2011GL048728>
- Zhang, Y., Seidel, D. J., Golaz, J. C., Deser, C., & Tomas, R. A. (2011). Climatological characteristics of Arctic and Antarctic surface-based inversions. *Journal of Climate*, 24(19), 5167–5186. <https://doi.org/10.1175/2011JCLI4004.1>
- Zhao, Y., & Sushama, L. (2020). Aircraft Takeoff Performance in a Changing Climate for Canadian Airports. *Atmosphere* . <https://doi.org/10.3390/atmos11040418>